Parameter-free effective field theory calculation for the solar proton-fusion and hep processes

T.-S. Park,[1,2,3] L. E. Marcucci,[4,5] R. Schiavilla,[6,7] M. Viviani,[5,4] A. Kievsky,[5,4] S. Rosati,[5,4] K. Kubodera,[1,2] D.-P. Min,[8] and M. Rho[1,9]

[1]*School of Physics, Korea Institute for Advanced Study, Seoul 130-012, Korea*
[2]*Department of Physics and Astronomy, University of South Carolina, Columbia, South Carolina 29208*
[3]*Department of Physics and Research Institute for Basic Sciences, Pusan National University, Busan 609-735, Korea*
[4]*Department of Physics, University of Pisa, I-56100 Pisa, Italy*
[5]*INFN, Sezione di Pisa, I-56100 Pisa, Italy*
[6]*Department of Physics, Old Dominion University, Norfolk, Virginia 23529*
[7]*Jefferson Lab, Newport News, Virginia 23606*
[8]*Department of Physics, Seoul National University, Seoul 151-742, Korea*
[9]*Service de Physique Théorique, CEA/DSM/SPhT, Unité de Recherche Associé au CNRS, CEA/Saclay, F-91191 Gif-sur-Yvette Cédex, France*

(Received 24 July 2001; revised manuscript received 23 December 2002; published 22 May 2003)

Spurred by the recent complete determination of the weak currents in two-nucleon systems up to $\mathcal{O}(Q^3)$ in heavy-baryon chiral perturbation theory, we carry out a parameter-free calculation of the threshold S factors for the solar pp (proton-fusion) and hep processes in an effective field theory (EFT) that *combines* the merits of the standard nuclear physics method and systematic chiral expansion. The power of the EFT adopted here is that one can correlate in a unified formalism the weak-current matrix elements of two-, three-, and four-nucleon systems. Using the tritium β-decay rate as an input to fix the only unknown parameter in the theory, we can evaluate the threshold S factors with drastically improved precision; the results are $S_{pp}(0)=3.94\times(1\pm0.004)\times10^{-25}$ MeV b and $S_{\rm hep}(0)=(8.6\pm1.3)\times10^{-20}$ keV b. The dependence of the calculated S factors on the momentum cutoff parameter Λ has been examined for a physically reasonable range of Λ. This dependence is found to be extremely small for the pp process, and to be within acceptable levels for the hep process, substantiating the consistency of our calculational scheme.

DOI: 10.1103/PhysRevC.67.055206 PACS number(s): 12.39.Fe, 24.85.+p, 26.20.+f, 26.65.+t

I. INTRODUCTION

The standard approach to nuclear physics [1] anchored on wave functions obtained from the Schrödinger (or Lippman-Schwinger) equation with ''realistic'' phenomenological potentials has scored impressive quantitative successes in describing systems with two or more nucleons, achieving in some cases accuracy that defies the existing experimental precision. We refer to this approach as SNPA (standard nuclear physics approach). The advent of quantum chromodynamics (QCD) as *the* theory of strong interactions raises a logical question: What is the status of SNPA in the context of the fundamental theory QCD? Put more bluntly, is SNPA (despite its undeniable success) just a model-dependent approach unrelated to the fundamental theory? In our view this is one of the most important issues in nuclear physics today. In this paper we investigate a possible way to identify SNPA as a *legitimate* component in the general edifice of QCD. We describe an attempt to find a scheme which includes SNPA as an approximation, and which allows us to control and evaluate correction terms. Such a systematic treatment equipped with error estimation, which is not feasible with SNPA alone, can be profitably studied with the effective field theory (EFT) of QCD. We study here a formalism which exploits simultaneously the merit of EFT in classifying interaction vertices unambiguously, and the high accuracy of nuclear wave functions available in SNPA. We demonstrate that this formalism enables us to make parameter-free *predictions* with accompanying error estimates for electroweak transitions in light nuclei. For a variant approach towards the EFT description of nuclear matter and heavy nuclei, we refer to Refs. [2–5].

To be concrete, we shall consider the following two solar nuclear fusion processes

$$pp:\ \ p+p\rightarrow d+e^{+}+\nu_e\,, \tag{1}$$

$$\text{hep:}\ \ p+{}^{3}\text{He}\rightarrow{}^{4}\text{He}+e^{+}+\nu_e\,. \tag{2}$$

We stress that in our EFT approach these processes involving different numbers of nucleons can be treated on the same footing. A concise account of the present study was previously given in Ref. [6] for the pp process and in Ref. [7] for the hep process.

The reactions (1) and (2) figure importantly in astrophysics and particle physics; they have much bearing upon issues of great current interest such as, for example, the solar neutrino problem and nonstandard physics in the neutrino sector. Since the thermal energy of the interior of the Sun is of the order of keV, and since no experimental data is available for such low-energy regimes, one must rely on theory for determining the astrophysical S factors of the solar nuclear processes. Here we concentrate on the threshold S factor $S(0)$ for the reactions (1) and (2). The necessity of a very accurate estimate of the threshold S factor for the pp process $S_{pp}(0)$ comes from the fact that pp fusion essentially governs the solar burning rate and the vast majority of the solar neutrinos come from this reaction. Meanwhile, the hep process is im-

portant in a different context. The hep reaction can produce the highest-energy solar neutrinos with their spectrum extending beyond the maximum energy of the ^{8}B neutrinos. Therefore, even though the flux of the hep neutrinos is small, there can be, at some level, a significant distortion of the higher end of the ^{8}B neutrino spectrum due to the hep neutrinos. This change can influence the interpretation of the results of a recent Super-Kamiokande experiment that have generated many controversies related to neutrino oscillations [8,9]. To address these issues quantitatively, a reliable estimate of $S_{\rm hep}(0)$ is indispensable.

The primary amplitudes for both the pp and hep processes are of the Gamow-Teller (GT) type ($\Delta J=1$, no parity change). Since the single-particle GT operator is well known at low energy, a major theoretical task is the accurate estimation of the meson-exchange current (MEC) contributions. The nature of a specific challenge involved here can be elucidated in terms of the *chiral filter* picture. If the MEC in a given transition receives an unsuppressed contribution from a one-soft-pion exchange diagram, then we can take advantage of the fact that the soft-pion-exchange MEC is uniquely dictated by chiral symmetry [10,11] and that there is a mechanism (called the chiral filter mechanism) that suppresses higher chiral-order terms [12,13]. We refer to a transition amplitude to which the chiral filter mechanism is applicable (not applicable) as a chiral-protected (chiral-unprotected) case. It is known that the space component of the vector current and the time component of the axial current are chiral protected, whereas the time component of the vector current and the space component of the axial current are chiral unprotected (see below). This implies among other things that the isovector $M1$ and axial-charge transitions are chiral protected [14,15], but that the GT transition is chiral unprotected. This feature renders the estimation of the GT amplitude a more subtle problem; the physics behind it is that MEC here receives significant short-ranged contributions the strength of which cannot be determined by chiral symmetry alone.

The difficulty becomes particularly pronounced for the hep process for the following reasons. First, the one-body (1B) GT matrix element for the hep process is strongly suppressed due to the symmetries of the initial and final state wave functions. Secondly, as pointed out in Refs. [16] (referred to as ''CRSW91'') and [17] (referred to as ''SWPC92''), the main two-body (2B) corrections to the ''leading'' 1B GT term tend to come with the opposite sign causing a large cancellation. A recent detailed SNPA calculation by Marcucci *et al.* [18], hereafter referred to as MS-VKRB, has reconfirmed this substantial cancellation between the 1B and 2B contributions. The 2B terms therefore need to be calculated with great precision, which is a highly nontrivial task. Indeed, an accurate evaluation of the hep rate has been a long-standing challenge in nuclear physics [19]. The degree of this difficulty may be appreciated by noting that theoretical estimates of the hep S factor have varied by orders of magnitude in the literature.

As mentioned, for accurate estimation of the GT transition amplitude, it is imperative to have good theoretical control of short-distance physics. A first-principle approach based on EFT should provide a valuable insight in this regard. Here we build on a formalism of this kind developed in Refs. [13,20]. In this formalism, [21], electroweak transition operators are systematically constructed using heavy-baryon chiral perturbation theory (HBχPT), and the corresponding nuclear matrix elements are evaluated with the use of wave functions generated by a state-of-the-art SNPA calculation. This is a hybrid approach in that, formally speaking, there is a mismatch between the treatments of transition operators and wave functions. However, we implement in our formalism a feature that allows us to reduce the practical consequences of this mismatch down to sufficiently low levels. To emphasize this feature, we refer to our present approach as EFT*.

The starting point of EFT* is the observation that, to high accuracy, the leading-order 1B operators in SNPA and EFT (HBχPT) are identical, and that their matrix elements can be reliably estimated with the use of realistic SNPA wave functions for the initial and final nuclear states. Next we note [20] that 2B transition operators in HBχPT are uniquely given by irreducible diagrams in Weinberg's counting scheme [22,23]. The long-range 2B contributions are in fact identical for both SNPA and EFT, as they are strongly constrained by chiral symmetry. It is short-range contributions that introduce model dependence in SNPA. EFT allows us to write down, for a given chiral order, the most general set of operators that govern short-distance physics as

$$\mathcal{O}_{\rm short}=\sum_{i=1}^{N} c_i\mathcal{O}_i\,, \tag{3}$$

where $\mathcal{O}_i$ is a zero-range operator (which may involve a derivative operator) and c_i is the corresponding low-energy constant (LEC); N is a finite number that depends on the chiral order under consideration. The c_i's, which should in principle be derivable from QCD, are in practice determined by fitting empirical data. Now, a nuclear matrix element in EFT* is obtained by sandwiching the EFT-controlled transition operator between the relevant SNPA wave functions. This means that, if two (or more) observables belonging to the same nucleus or to neighboring nuclei are sensitive to $\mathcal{O}_{\rm short}$, they can be related via EFT*. If the experimental value of one of those observables is known, the other(s) can be predicted. Correlating two (or more) observables in this manner is expected to significantly reduce the practical consequences of the afore-mentioned ''mismatch problem.'' The basic soundness of this approach has been proven for the $n+p\to d+\gamma$ process [14,24] and several other processes [25]. We emphasize that EFT*, which takes into account short-distance physics consistently, should be distinguished from naive hybrid models, which lack this feature. Having described EFT* in rather general terms, we give in the next two paragraphs more specific aspects pertaining to the pp and hep processes.

An early HBχPT study of the pp process was made in Ref. [26] (hereafter referred to as PKMR98) by four of the authors. The calculation in PKMR98 was carried out up to next-to-next-to-next-to-leading order (N^{3}LO) in chiral counting (see below). At N^{3}LO, two-body MEC begin to contrib-

ute, and there appears one unknown parameter in the chiral Lagrangian contributing to the MEC. This unknown constant, called $\hat{d}^R$ in Ref. [26], represents the strength of a four-nucleon-axial-current contact interaction. In Ref. [26], since no method was known to fix the value of $\hat{d}^R$, the $\hat{d}^R$ term was simply ignored by invoking a qualitative argument that the short-range repulsive core would strongly suppress its contribution. Due to uncertainties associated with this argument, Ref. [26] was unable to corroborate or exclude the result of the latest SNPA calculation [27], $\delta_{2B}=0.5-0.8$ %, where δ_{2B} is the ratio of the contribution of the two-body MEC to that of the one-body current (see below).

The situation can be greatly improved by using EFT*. As first discussed in Refs. [6,7] and as will be expounded here, the crucial point is that exactly the same combination of counterterms that defines the constant $\hat{d}^R$ enters into the Gamow-Teller (GT) matrix elements that feature in pp fusion, tritium β decay, the hep process, μ capture on a deuteron, and ν–d scattering and that the short-range interaction involving the constant $\hat{d}^R$ is expected to be ''universal,'' that is, A independent. Therefore, assuming that three- and four-body currents can be ignored (which we will justify *a posteriori*), if the value of $\hat{d}^R$ can be fixed using one of the above processes, we can make a totally parameter-free prediction for the GT matrix elements of the other processes. Indeed, the existence of accurate experimental data for the tritium β-decay rate Γ_β^t and the availability of extremely well tested realistic wave functions for the $A=3$ nuclear systems allow us to carry out this program. In the present work we determine the value of $\hat{d}^R$ from Γ_β^t and perform parameter-free EFT-based calculations of $S_{pp}(0)$ and $S_{\rm hep}(0)$.

As described below, our scheme has a cutoff parameter Λ, which defines the energy/momentum cutoff scale of EFT below which reside the chosen explicit degrees of freedom [28]. Obviously, in order for our result to be physically acceptable, its cutoff dependence must be under control. In our scheme, for a given value of Λ in a physically reasonable range (to be discussed later), $\hat{d}^R$ is determined to reproduce Γ_β^t; thus $\hat{d}^R$ is a function of Λ. According to the premise of EFT, even if $\hat{d}^R$ itself is Λ dependent, physical observables (in our case the S factors) should be independent of Λ as required by renormalization-group invariance. We shall show that our results meet this requirement to a satisfactory degree. The robustness of our calculational results against changes in Λ allows us to make predictions on $S_{pp}(0)$ and $S_{\rm hep}(0)$ with much higher precision than hitherto achieved. Thus we predict $S_{pp}(0)=3.94\times(1\pm0.004)\times10^{-25}$ MeV b and $S_{\rm hep}(0)=(8.6\pm1.3)\times10^{-20}$ keV b.

The remainder of this article is organized as follows. In Sec. II we briefly explain our formalism; in particular, we describe the relevant transition operators derived in HBχPT. The determination of $\hat{d}^R$ is described in Sec. III. Section IV presents the calculation of $S_{pp}(0)$, while Sec. V is concerned with the estimation of $S_{\rm hep}(0)$. Section VI is devoted to discussion and conclusions. We have made the explanation of the formalism in the text as brief and focused as possible, relegating most technical details to the Appendixes.

II. FORMALISM

We sketch here the basic elements of our formalism. The explicit degrees of freedom taken into account in our scheme are the nucleon and the pion, with all other degrees of freedom [ρ and ω mesons, $\Delta(1232)$, etc.] integrated out. The HBχPT Lagrangian can be written as

$$\mathcal{L}=\sum_\lambda \mathcal{L}_\lambda=\mathcal{L}_0+\mathcal{L}_1+\cdots, \tag{4}$$

with the chiral order λ defined as

$$\lambda\equiv d+e+\frac{n}{2}-2, \tag{5}$$

where d, e, and n are, respectively, the numbers of derivatives (the pion mass counted as one derivative), external fields and nucleon lines belonging to a vertex. Chiral symmetry requires $\lambda\geqslant0$. The leading-order Lagrangian is given by

$$\mathcal{L}_0=\bar{B}[iv\cdot D+2ig_A S\cdot\Delta]B-\frac{1}{2}\sum_A C_A(\bar{B}\Gamma_A B)^2$$
$$+f_\pi^2\mathrm{Tr}(i\Delta^\mu i\Delta_\mu)+\frac{f_\pi^2}{4}\mathrm{Tr}(\chi_+), \tag{6}$$

where B is the nucleon field in HBχPT; $g_A=1.2670\pm0.0035$ is the axial-vector coupling constant [29], and $f_\pi=92.4$ MeV is the pion decay constant. Furthermore

$$D_\mu B=(\partial_\mu+\Gamma_\mu)B,$$
$$\Gamma_\mu=\frac{1}{2}[\xi^\dagger,\ \partial_\mu\xi]-\frac{i}{2}\xi^\dagger R_\mu\xi-\frac{i}{2}\xi L_\mu\xi^\dagger,$$
$$\Delta_\mu=\frac{1}{2}[\xi^\dagger,\ \partial_\mu\xi]+\frac{i}{2}\xi^\dagger R_\mu\xi-\frac{i}{2}\xi L_\mu\xi^\dagger,$$
$$\chi_+=\xi^\dagger\chi\xi^\dagger+\xi\chi^\dagger\xi, \tag{7}$$

with

$$\xi=\sqrt{\Sigma}=\exp\left(i\frac{\vec{\tau}\cdot\vec{\pi}}{2f_\pi}\right). \tag{8}$$

$R_\mu\equiv(\tau^a/2)(\mathcal{V}_\mu^a+\mathcal{A}_\nu^a)$ and $L_\mu=(\tau^a/2)(\mathcal{V}_\mu^a-\mathcal{A}_\nu^a)$ denote external gauge fields, and χ is proportional to the quark mass matrix. If we neglect the small isospin-symmetry breaking, then $\chi=m_\pi^2$ (in the absence of external scalar and pseudoscalar fields). For convenience, we work in the reference frame in which the four velocity v^μ and the spin operator S^μ are

$$v^\mu=(1,\ \mathbf{0}) \quad \text{and} \quad S^\mu=\left(0,\ \frac{\boldsymbol{\sigma}}{2}\right). \tag{9}$$

The NLO Lagrangian (the so-called ''$1/m$'' term) in the one-nucleon sector is given in Ref. [30], while that in the two-nucleon sector is given in Refs. [31,32]. With four-fermion contact terms included, the Lagrangian takes the form

$$\begin{aligned}\mathcal{L}_1=\overline{B}\Bigg\{&\frac{v^\mu v^\nu-g^{\mu\nu}}{2m_N}D_\mu D_\nu+4c_3 i\Delta i\Delta\cdot\Delta\\&+\left(2c_4+\frac{1}{2m_N}\right)[S^\mu,\ S^\nu][i\Delta_\mu,\ i\Delta_\nu]\\&-i\frac{1+c_6}{m_N}[S^\mu,\ S^\nu]f^+_{\mu\nu}\Bigg\}B-4id_1\overline{B}S\Delta B\,\overline{B}B\\&+2id_2\epsilon^{abc}\epsilon_{\mu\nu\lambda\delta}v^\mu\Delta^{\nu,a}\overline{B}S^\lambda\tau^b B\ \ \overline{B}S^\delta\tau^c B+\cdots,\end{aligned} \tag{10}$$

where $m_N\simeq 939$ MeV is the nucleon mass, and

$$\begin{aligned}f^+_{\mu\nu}=&\xi(\partial_\mu L_\nu-\partial_\nu L_\mu-i[L_\mu,\ L_\nu])\xi^\dagger\\&+\xi^\dagger(\partial_\mu R_\nu-\partial_\nu R_\mu-i[R_\mu,\ R_\nu])\xi,\end{aligned} \tag{11}$$

$\epsilon_{0123}=1$, and $\Delta_\mu=(\tau^a/2)\Delta^a_\mu$. We have shown here only those terms which are directly relevant to our present study. The dimensionless LECs, $\hat{c}$'s and $\hat{d}$'s, are defined as

$$c_{3,4}=\frac{1}{m_N}\hat{c}_{3,4},\quad d_{1,2}=\frac{g_A}{m_N f_\pi^2}\hat{d}_{1,2}. \tag{12}$$

We now consider the chiral counting of the electroweak currents (see the Appendixes for details). In the present scheme it is sufficient to focus on ''irreducible graphs'' in Weinberg's classification [22]. Irreducible graphs are organized according the chiral index ν given by

$$\nu=2(A-C)+2L+\sum_i \nu_i, \tag{13}$$

where A is the number of nucleons involved in the process, C the number of disconnected parts, and L the number of loops; ν_i is the chiral index λ, Eq. (5), of the ith vertex. One can show that a diagram characterized by Eq. (13) involves an n_B-body transition operator, where $n_B\equiv A-C+1$. The physical amplitude is expanded with respect to ν. As explained at length in the Appendix, the leading-order one-body GT operator belongs to $\nu=0$. Compared with this operator, a Feynman diagram with a chiral index ν is suppressed by a factor of $(Q/\Lambda_\chi)^\nu$, where Q is a typical three-momentum scale or the pion mass, and $\Lambda_\chi\sim$ 1 GeV is the chiral scale [33]. In our case it is important to take into account the kinematic suppression of the time component of the nucleon four-momentum. We note [34]

$$v\cdot p_l\sim v\cdot p_l'\sim v\cdot k_l\sim\frac{Q^2}{m_N}, \tag{14}$$

TABLE I. Contributions from each type of current at $\boldsymbol{q}=\mathbf{0}$. The entry of ''$-$'' indicates the absence of contribution. ''1B-RC'' stands for relativistic corrections to the one-body operators, and ''2B-1L'' for one-loop two-body contributions including counter-term contributions.

J^μ	LO	NLO	N^{2}LO	N^{3}LO	N^{4}LO
$\boldsymbol{A}$	1B	$-$	1B-RC	2B	1B-RC, 2B-1L, and 3B
A^0	$-$	1B	2B	1B-RC	1B-RC, 2B-1L
$\boldsymbol{V}$	$-$	1B	2B	1B-RC	1B-RC, 2B-1L
V^0	1B	$-$	$-$	2B	1B-RC, 2B-1L and 3B

where p_l^μ ($p_l'^\mu$) denotes the initial (final) momentum of the lth nucleon, and $k_l^\mu\equiv(p_l'-p_l)^\mu$. Therefore, each appearance of $v\cdot p_l$, $v\cdot p_l'$, or $v\cdot k_l$ carries two powers of Q instead of one, which implies that ν increases by two units rather than one. It is also to be noted that, if we denote by $q^\mu=(q_0,\boldsymbol{q})$ the momentum transferred to the leptonic pair in Eqs. (1), (2), then $q_0\sim|\boldsymbol{q}|\sim Q^2/\Lambda_\chi\sim\mathcal{O}(Q^2)$ rather than $\mathcal{O}(Q)$ as naive counting would suggest. These features turn out to simplify our calculation considerably.

In this paper, as far as the main calculation is concerned, we shall limit ourselves to N^{3}LO; for certain discussions, however, we shall consider operators belonging to N^{4}LO as well.

We now describe the derivation of one-body (1B) and two-body (2B) current operators with due consideration of chiral counting. The current in momentum space is written as

$$J^\mu(\boldsymbol{q})=V^\mu(\boldsymbol{q})+A^\mu(\boldsymbol{q})=\int d\boldsymbol{x}\ \ e^{-i\boldsymbol{q}\cdot\boldsymbol{x}}J^\mu(\boldsymbol{x}). \tag{15}$$

When necessity arises to distinguish the space and time components of the currents, we use the notations

$$V^\mu=(V^0,\boldsymbol{V})\quad A^\mu=(A^0,\boldsymbol{A}). \tag{16}$$

For the clarity of presentation, we first give a summary chart of the basic chiral counting characteristics of the relevant currents, and then provide more detailed explanations in the remainder of this section and in the Appendixes. The chiral counting of the electroweak currents is summarized in Table I, where the nonvanishing contributions at $\boldsymbol{q}=\mathbf{0}$ are indicated [35].

We now discuss the entries of this table order by order.

$\nu=0$. One-body $\boldsymbol{A}$ and V^0: $\boldsymbol{A}$ gives the Gamow-Teller (GT) operator, while V^0 is responsible for the charge operator.

$\nu=1$. One-body A^0 and $\boldsymbol{V}$: A^0 gives the axial-charge operator while $\boldsymbol{V}$ gives the $M1$ operator.

$\nu=2$. Two-body tree current with $\nu_i=0$ vertices, namely, the soft-pion-exchange current. This is a leading correction to the one-body $M1$ and axial-charge operators carrying an odd orbital angular momentum.

$\nu=3$. Two-body tree currents with $\Sigma_i \nu_i=1$, which correspond to the hard-pion current, considered in CRSW91 [16] and SWPC92 [17]. These are leading corrections to the GT and V^0 operators carrying an even orbital angular momentum.

$\nu=4$. All the components of the electroweak current receive contributions of this order. They consist of two-body one-loop corrections as well as leading-order (tree) three-body corrections. Among the three-body currents, however, there are no six-fermion contact terms proportional to $(\bar{N}N)^3$, because there is no derivative at the vertex and hence no external field.

It is noteworthy that the counting rule for $\boldsymbol{V}$ is the same as for A^0, and the counting rules for V^0 and $\boldsymbol{A}$ are the same. The behavior of $\boldsymbol{V}$ and A^0 summarized in Table I represents the chiral filter mechanism [12], and $\boldsymbol{V}$ and A^0 are referred to as chiral-filter-protected currents. By contrast, V^0 and $\boldsymbol{A}$ belong to chiral-filter-unprotected currents.

We now discuss the explicit expressions for the relevant currents. For the 1B currents, for both the vector and axial cases, one can simply carry over the expressions obtained in MSVKRB. Up to N^{3}LO, the 1B currents in coordinate representation are given as

$$V_l^0=\tau_l^- e^{-i\boldsymbol{q}\cdot\boldsymbol{r}_l}\left[1+i\boldsymbol{q}\cdot\boldsymbol{\sigma}_l\times\boldsymbol{p}_l\frac{2\mu_V-1}{4m_N^2}\right],$$

$$\boldsymbol{V}_l=\tau_l^- e^{-i\boldsymbol{q}\cdot\boldsymbol{r}_l}\left[\frac{\bar{\boldsymbol{p}}_l}{m_N}\left(1-\frac{\bar{\boldsymbol{p}}_l^2}{2m_N^2}\right)+i\frac{\mu_V}{2m_N}\boldsymbol{q}\times\boldsymbol{\sigma}_l+i\boldsymbol{\sigma}_l\times\bar{\boldsymbol{p}}_l q_0\frac{2\mu_V-1}{4m_N^2}\right],$$

$$A_l^0=-g_A\tau_l^- e^{-i\boldsymbol{q}\cdot\boldsymbol{r}_l}\left[\frac{\boldsymbol{\sigma}_l\cdot\bar{\boldsymbol{p}}_l}{m_N}\left(1-\frac{\bar{\boldsymbol{p}}_l^2}{2m_N^2}\right)\right],$$

$$\boldsymbol{A}_l=-g_A\tau_l^- e^{-i\boldsymbol{q}\cdot\boldsymbol{r}_l}\left[\boldsymbol{\sigma}_l+\frac{2(\bar{\boldsymbol{p}}_l\boldsymbol{\sigma}_l\cdot\bar{\boldsymbol{p}}_l-\boldsymbol{\sigma}_l\bar{\boldsymbol{p}}_l^2)+i\boldsymbol{q}\times\bar{\boldsymbol{p}}_l}{4m_N^2}\right], \tag{17}$$

where $\mu_V\simeq 4.70$ is the isovector anomalous magnetic moment of the nucleon and $\boldsymbol{p}_l=-i\nabla_l$ and $\bar{\boldsymbol{p}}_l=-(i/2)(\vec{\nabla}_l-\overleftarrow{\nabla}_l)$ act on the wave functions. Equation (17) gives the isospin-lowering currents

$$J_\mu\equiv J_\mu^{a=1}-iJ_\mu^{a=2} \tag{18}$$

and $\tau_l^-\equiv\frac{1}{2}(\tau_l^x-i\tau_l^y)$.

We next discuss the 2B currents. The expressions for the $\boldsymbol{V}_{2\mathrm{B}}$ and $A_{2\mathrm{B}}^0$ operators can be found in Refs. [20,36]. The $V_{2\mathrm{B}}^0$ operator does not appear up to the order under consideration. The derivation of the 2B axial current $\boldsymbol{A}_{2\mathrm{B}}$ in HBχPT is described in Appendix A. In momentum space, $\boldsymbol{A}_{2\mathrm{B}}$ reads

$$\boldsymbol{A}_{2\mathrm{B}}=\sum_{l<m}^{A}\boldsymbol{A}_{lm},$$

$$\boldsymbol{A}_{12}=\frac{g_A}{2m_N f_\pi^2}\frac{1}{m_\pi^2+\boldsymbol{k}^2}\left[-\frac{i}{2}\tau_\times^-\boldsymbol{p}(\boldsymbol{\sigma}_1-\boldsymbol{\sigma}_2)\cdot\boldsymbol{k}+4\hat{c}_3\boldsymbol{k}\boldsymbol{k}\cdot(\tau_1^-\boldsymbol{\sigma}_1+\tau_2^-\boldsymbol{\sigma}_2)+\left(\hat{c}_4+\frac{1}{4}\right)\tau_\times^-\boldsymbol{k}\times[\boldsymbol{\sigma}_\times\times\boldsymbol{k}]\right]+\frac{g_A}{m_N f_\pi^2}[2\hat{d}_1(\tau_1^-\boldsymbol{\sigma}_1+\tau_2^-\boldsymbol{\sigma}_2)+\hat{d}_2\tau_\times^a\boldsymbol{\sigma}_\times], \tag{19}$$

with $\boldsymbol{k}\equiv(\boldsymbol{k}_2-\boldsymbol{k}_1)/2$, $\boldsymbol{k}_l\equiv\boldsymbol{p}_l'-\boldsymbol{p}_l$, $\boldsymbol{p}\equiv(\bar{\boldsymbol{p}}_1-\bar{\boldsymbol{p}}_2)/2$, $\bar{\boldsymbol{p}}_l\equiv(\boldsymbol{p}_l+\boldsymbol{p}_l')/2$, $\tau_l^-\equiv\frac{1}{2}(\tau_l^x-i\tau_l^y)$, $\tau_\times^a\equiv(\tau_1\times\tau_2)^x-i(\tau_1\times\tau_2)^y$, and similarly for $\sigma_\times$; $\hat{c}$'s and $\hat{d}$'s are the LECs explained in PKMR98. The values of $\hat{c}$'s in Eq. (19) have been determined from π-N data [37]: $\hat{c}_3=-3.66\pm0.08$ and $\hat{c}_4=2.11\pm0.08$. The two constants $\hat{d}_1$ and $\hat{d}_2$ remain to be fixed but it turns out (see Appendix C 2) that, thanks to Fermi-Dirac statistics, only one combination of them

$$\hat{d}^R\equiv\hat{d}_1+2\hat{d}_2+\frac{1}{3}\hat{c}_3+\frac{2}{3}\hat{c}_4+\frac{1}{6} \tag{20}$$

is relevant in the present context [38].

It should be noted that the two-body currents given in Eq. (19) are valid only up to a certain cutoff Λ. This implies that, when we go to coordinate space, the currents must be regulated. This is a key point in our approach. Specifically, in performing Fourier transformation to derive the r-space representation of a transition operator, we use the Gaussian regularization (see Appendix C). This is, to good accuracy, equivalent to replacing the delta and Yukawa functions with the corresponding regulated functions

$$\delta_\Lambda^{(3)}(r)\equiv\int\frac{d^3\boldsymbol{k}}{(2\pi)^3}S_\Lambda^2(\boldsymbol{k}^2)e^{i\boldsymbol{k}\cdot\boldsymbol{r}},$$

$$y_{0\Lambda}^\pi(r)\equiv\int\frac{d^3\boldsymbol{k}}{(2\pi)^3}S_\Lambda^2(\boldsymbol{k}^2)e^{i\boldsymbol{k}\cdot\boldsymbol{r}}\frac{1}{\boldsymbol{k}^2+m_\pi^2},$$

$$y_{1\Lambda}^\pi(r)\equiv-r\frac{\partial}{\partial r}y_{0\Lambda}^\pi(r),$$

$$y_{2\Lambda}^\pi(r)\equiv\frac{1}{m_\pi^2}r\frac{\partial}{\partial r}\frac{1}{r}\frac{\partial}{\partial r}y_{0\Lambda}^\pi(r), \tag{21}$$

where the cutoff function $S_\Lambda(\boldsymbol{k}^2)$ is defined as

$$S_\Lambda(\boldsymbol{k}^2)=\exp\left(-\frac{\boldsymbol{k}^2}{2\Lambda^2}\right). \tag{22}$$

The resulting r-space expressions of the currents in the center-of-mass (c.m.) frame that are of N^{3}LO are

$$\boldsymbol{V}_{12}(\boldsymbol{r}) = -\frac{g_A^2 m_\pi^2}{12 f_\pi^2}\tau_\times^- \boldsymbol{r}[\boldsymbol{\sigma}_1\cdot\boldsymbol{\sigma}_2 y_{0\Lambda}^\pi(r) + S_{12} y_{2\Lambda}^\pi(r)] - i\frac{g_A^2}{8 f_\pi^2}\boldsymbol{q}\times\left[\boldsymbol{\mathcal{O}}_\times y_{0\Lambda}^\pi(r) + \left(\boldsymbol{\mathcal{T}}_\times - \frac{2}{3}\boldsymbol{\mathcal{O}}_\times\right) y_{1\Lambda}^\pi(r)\right],$$

$$A_{12}^0(\boldsymbol{r}) = -\frac{g_A}{4 f_\pi^2}\tau_\times^-\left[\frac{\boldsymbol{\sigma}_+\cdot\hat{\boldsymbol{r}}}{r} + \frac{i}{2}\boldsymbol{q}\cdot\hat{\boldsymbol{r}}\boldsymbol{\sigma}_-\cdot\hat{\boldsymbol{r}}\right] y_{1\Lambda}^\pi(r),$$

$$\boldsymbol{A}_{12}(\boldsymbol{r}) = -\frac{g_A m_\pi^2}{2 m_N f_\pi^2}\left[\left[\frac{\widehat{c_3}}{3}(\boldsymbol{\mathcal{O}}_+ + \boldsymbol{\mathcal{O}}_-) + \frac{2}{3}\left(\hat{c}_4 + \frac{1}{4}\right)\times\boldsymbol{\mathcal{O}}_\times\right] y_{0\Lambda}^\pi(r) + \left[\hat{c}_3(\boldsymbol{\mathcal{T}}_+ + \boldsymbol{\mathcal{T}}_-) - \left(\hat{c}_4 + \frac{1}{4}\right)\times\boldsymbol{\mathcal{T}}_\times\right] y_{2\Lambda}^\pi(r)\right] + \frac{g_A}{2 m_N f_\pi^2}\left[\frac{1}{2}\tau_\times^-(\overline{\boldsymbol{p}_1}\boldsymbol{\sigma}_2\cdot\hat{\boldsymbol{r}} + \overline{\boldsymbol{p}_2}\boldsymbol{\sigma}_1\cdot\hat{\boldsymbol{r}})\frac{y_{1\Lambda}^\pi(r)}{r} + \delta_\Lambda(r)\hat{d}^R\boldsymbol{\mathcal{O}}_\times\right], \tag{23}$$

where $\boldsymbol{r}=\boldsymbol{r}_1-\boldsymbol{r}_2$, $S_{12}=3\boldsymbol{\sigma}_1\cdot\hat{\boldsymbol{r}}\boldsymbol{\sigma}_2\cdot\hat{\boldsymbol{r}}-\boldsymbol{\sigma}_1\cdot\boldsymbol{\sigma}_2$, and $\boldsymbol{\mathcal{O}}_\odot^k \equiv \tau_\odot^-\boldsymbol{\sigma}_\odot^k$, $\boldsymbol{\mathcal{O}}_\odot \equiv \tau_\odot^-\boldsymbol{\sigma}_\odot$, $\boldsymbol{\mathcal{T}}_\odot \equiv \hat{\boldsymbol{r}}\hat{\boldsymbol{r}}\cdot\boldsymbol{\mathcal{O}}_\odot - \frac{1}{3}\boldsymbol{\mathcal{O}}_\odot$, $\odot = \pm, \times, \tau_\odot^- \equiv (\tau_1\odot\tau_2)^- \equiv (\tau_1\odot\tau_2)^x - i(\tau_1\odot\tau_2)^y$, and $\boldsymbol{\sigma}_\odot \equiv (\boldsymbol{\sigma}_1\odot\boldsymbol{\sigma}_2)$. We emphasize again that $\boldsymbol{A}_{12}$ in Eq. (23) contains only one unknown LEC $\hat{d}^R$ that needs to be fixed using an empirical input. As mentioned in Sec. I, we choose here to determine $\hat{d}^R$ using the experimental value of Γ_β^t.

III. DETERMINATION OF $\hat{d}^R$

The cutoff parameter Λ characterizes the energy-momentum scale of our EFT. A reasonable range of Λ may be inferred as follows. According to the general *tenet* of χPT, Λ larger than $\Lambda_\chi \simeq 4\pi f_\pi \simeq m_N$ has no physical meaning. Meanwhile, since the pion is an explicit degree of freedom in our scheme, Λ should be much larger than the pion mass to ascertain that genuine low-energy contributions are properly included. These considerations lead us to adopt $\Lambda = 500$–800 MeV as a natural range.

In the present work we use as representative values $\Lambda = 500$, 600, and 800 MeV, and for each of these values of Λ we adjust $\hat{d}^R$ to reproduce the experimental value of Γ_β^t. With the use of the value of $\hat{d}^R$ so determined, we evaluate the pp and the hep amplitudes [39].

To determine $\hat{d}^R$ from Γ_β^t, we calculate Γ_β^t from the matrix elements of the current operators evaluated for accurate $A=3$ nuclear wave functions. We employ here the wave functions obtained in Refs. [18,40] using the correlated-hyperspherical-harmonics (CHH) method [41,42]. It is obviously important to maintain consistency between the treatments of the $A=2$, 3, and 4 systems. We shall use here the same Argonne v_{18} (AV18) potential [43] for all these nuclei. For the $A \geqslant 3$ systems we add the Urbana-IX (AV18/UIX) three-nucleon potential [44]. Furthermore, we apply the same regularization method to all the systems in order to control short-range physics in a consistent manner.

The values of $\hat{d}^R$ determined in this manner are

$$\hat{d}^R = 1.00 \pm 0.07 \quad \text{for} \quad \Lambda = 500 \ \text{MeV},$$
$$\hat{d}^R = 1.78 \pm 0.08 \quad \text{for} \quad \Lambda = 600 \ \text{MeV}, \tag{24}$$
$$\hat{d}^R = 3.10 \pm 0.10 \quad \text{for} \quad \Lambda = 800 \ \text{MeV},$$

where the errors correspond to the experimental uncertainty in Γ_β^t. Once $\hat{d}^R$ has been determined, we are in a position to make a parameter-free calculation of the transition amplitudes for pp and hep, which will be described in the next two sections.

IV. THE pp PROCESS

It is convenient to decompose the matrix element of the GT operator into one-body and two-body parts

$$\mathcal{M} = \mathcal{M}_{1\mathrm{B}} + \mathcal{M}_{2\mathrm{B}}. \tag{25}$$

We discuss them separately. In PKMR98, an extensive analysis was made of the leading-order (LO) one-body matrix element $\mathcal{M}_{1\mathrm{B}}^{C+N}$, with a focus on the connection between EFT and the effective range expansion. The results obtained with the AV18 potential [43] were

$$\mathcal{M}_{1\mathrm{B}}^{C+N} = (1 \mp 0.02\% \mp 0.07\% \mp 0.02\%) \times 4.859 \ \text{fm}, \tag{26}$$

where the errors are due to uncertainties in the scattering length and effective ranges. The ''full'' one-body contribution in PKMR98 includes the vacuum-polarization (VP) and two-photon-exchange (C2) contributions. In PKMR98, however, the one-body current due to the $1/m_N^2$ term in Eq. (A3) was ignored. Although this term is required for formal consistency, its numerical value turns out to be quite small, $\mathcal{M}_{1\mathrm{B}}^{1/m_N^2} = -0.006$ fm. In terms of the Λ_{pp} defined in Refs. [45,46] we have

$$\Lambda_{pp}^2 \equiv \frac{|a^C|^2\gamma^3}{2}\ A_S^2 \mathcal{M}_{1\mathrm{B}}^2 = 6.91 \tag{27}$$

for the central value, where a^C is the pp $^1\mathrm{S}_0$ scattering length, and γ and A_S are the wave number and S-wave normalization constant pertinent to the deuteron, respectively. This should be compared with 6.93 obtained in Ref. [26].

The properly regularized two-body GT matrix elements for the pp process read

TABLE II. The strength $\hat{d}^R$ of the contact term and the two-body GT matrix element $\mathcal{M}_{2B}$ for the pp process calculated for representative values of Λ.

Λ (MeV)	$\hat{d}^R$	$\mathcal{M}_{2B}$ (fm)
500	1.00 ± 0.07	$0.076 - 0.035\ \hat{d}^R \simeq 0.041 \pm 0.002$
600	1.78 ± 0.08	$0.097 - 0.031\ \hat{d}^R \simeq 0.042 \pm 0.002$
800	3.90 ± 0.10	$0.129 - 0.022\ \hat{d}^R \simeq 0.042 \pm 0.002$

$$\mathcal{M}_{2B} = \frac{2}{m_N f_\pi^2} \int_0^\infty dr \times \left\{ \frac{m_\pi^2}{3} \left(\hat{c}_3 + 2\hat{c}_4 + \frac{1}{2} \right) y_{0\Lambda}^\pi(r) u_d(r) u_{pp}(r) - \sqrt{2} \frac{m_\pi^2}{3} \left(\hat{c}_3 - \hat{c}_4 - \frac{1}{4} \right) y_{2\Lambda}^\pi(r) w_d(r) u_{pp}(r) + \frac{y_{1\Lambda}^\pi(r)}{12r} \left[[u_d(r) - \sqrt{2} w_d(r)] u'_{pp}(r) - [u'_d(r) - \sqrt{2} w'_d(r)] u_{pp}(r) + \frac{3\sqrt{2}}{r} w_d(r) u_{pp}(r) \right] - \hat{d}^R \delta_\Lambda^{(3)}(r) u_d(r) u_{pp}(r) \right\}, \tag{28}$$

where $u_d(r)$ and $w_d(r)$ are the S- and D-wave components of the deuteron wave function, and $u_{pp}(r)$ is the $^1S_0$ pp scattering wave (at zero relative energy). The results are given for the three representative values of Λ in Table II; for convenience, the values of $\hat{d}^R$ given in Eq. (24) are also listed. The table indicates that, although the value of $\hat{d}^R$ is sensitive to Λ, $\mathcal{M}_{2B}$ is amazingly stable against the variation of Λ within the stated range. In view of this high stability, we believe that we are on the conservative side in adopting the estimate $\mathcal{M}_{2B} = (0.039\text{–}0.044)$ fm. Since the leading single-particle term is independent of Λ, the total amplitude $\mathcal{M} = \mathcal{M}_{1B} + \mathcal{M}_{2B}$ is Λ independent to the same degree as $\mathcal{M}_{2B}$. The Λ independence of the physical quantity $\mathcal{M}$, which is in conformity with the tenet of EFT, is a crucial feature of the result in our present study. The relative strength of the two-body contribution as compared with the one-body contribution is

$$\delta_{2B} \equiv \frac{\mathcal{M}_{2B}}{\mathcal{M}_{1B}} = (0.86 \pm 0.05)\%. \tag{29}$$

We remark that the central value of δ_{2B} here is considerably smaller than the corresponding value $\delta_{2B} = 4\%$ in PKMR98. Furthermore, the uncertainty of $\pm 0.05\%$ in Eq. (29) is drastically smaller than the corresponding figure $\pm 4\%$ in PKMR98.

We now turn to the threshold S factor $S_{pp}(0)$. Adopting the value $G_V = (1.14939 \pm 0.00065) \times 10^{-5}\text{GeV}^{-2}$ [47], we obtain

$$S_{pp}(0) = 3.94 \times \left(\frac{1 + \delta_{2B}}{1.01} \right)^2 \left(\frac{g_A}{1.2670} \right)^2 \left(\frac{\Lambda_{pp}^2}{6.91} \right)^2 = 3.94 \times (1 \pm 0.0015 \pm 0.0010 \pm \varepsilon) \tag{30}$$

in units of 10^{-25} MeV b. Here the first error is due to uncertainties in the input parameters in the one-body part, while the second error represents the uncertainties in the two-body part; $\varepsilon (\approx 0.001)$ denotes possible uncertainties due to higher chiral order contributions (see below). To make a formally rigorous assessment of ε, we must evaluate loop corrections and higher-order counter terms. Although an N^{4}LO calculation would not involve any new unknown parameters, it is a nontrivial task. Furthermore, loop corrections necessitate a more elaborate regularization scheme since the naive cutoff regularization used here violates chiral symmetry at loop orders. (This difficulty, however, is not insurmountable.) These formal problems set aside, it seems reasonable to assess ε as follows. We first recall that both tritium β decay and solar pp fusion are dominated by the one-body GT matrix elements, the evaluation of which is extremely well controlled from the SNPA as well as EFT points of view. Therefore, the precision of our calculation is governed by the reliability of estimation of small corrections to the dominant one-body GT contribution. Now, we have seen that the results of the present N^{3}LO calculation nicely fit into the picture expected from the general premise of EFT: (i) the N^{3}LO contributions are indeed much smaller than the leading order term. (ii) The physical transition amplitude $\mathcal{M}$ does not depend on the cutoff parameter. Although these features do not constitute a formal proof of the convergence of the chiral expansion used here, it is *extremely unlikely* that higher order contributions be so large as to completely upset the physically reasonable behavior observed in the N^{3}LO calculation. It should therefore be safe to assign to ε an uncertainty comparable to the error estimate for the two-body part in Eq. (30); viz., $\varepsilon \approx 0.1$ %. In this connection we remark that an axial three-body MEC contribution to the ^{3}H GT matrix element was calculated explicitly in SNPA [18] and found to be negligible relative to the leading two-body mechanisms. This feature is consistent with the above argument since, in the context of EFT, the three-body MEC represents a higher-order effect subsumed in "ε" in Eq. (30).

Apart from the noticeable numerical differences between the present work and PKMR98, it is worth noting that short-range physics is much better controlled in EFT*. In the conventional treatment of MEC, one derives the coordinate space representation of a MEC operator by applying ordinary Fourier transformation (with no restriction on the range of the momentum variable) to the amplitude obtained in momentum space; this corresponds to setting $\Lambda = \infty$ in Eq. (22). In PKMR98, where this familiar method is adopted, the $\hat{d}^R$ term appears in the zero-range form $\hat{d}^R \delta(r)$. PKMR98 chose to introduce short-range repulsive correlation with hard-core radius r_C and eliminate the $\hat{d}^R \delta(r)$ term *by hand*. The remaining finite-range terms were evaluated as functions of r_C. $\mathcal{M}_{2B}$ calculated this way exhibited substantial r_C dependence, indicating that short-range physics was not well con-

TABLE III. Values of $\hat{d}^R$ and $\overline{L_1}(q;A)$ (in fm$^{3/2}$) for the hep process calculated as functions of the cutoff Λ. The individual contributions from the one-body (1B) and two-body (2B) operators are also listed.

Λ (MeV)	500	600	800
$\hat{d}^R$	1.00 ± 0.07	1.78 ± 0.08	3.90 ± 0.10
$\overline{L_1}(q;A)$	-0.032	-0.029	-0.022
1B	-0.081	-0.081	-0.081
2B (without $\hat{d}^R$)	0.093	0.122	0.166
2B ($\propto\hat{d}^R$)	-0.044	-0.070	-0.107
2B total	0.049	0.052	0.059

trolled. Inclusion of the $\hat{d}^R$ term, with its strength renormalized as described here, properly takes into account the short-range physics inherited from the integrated out degrees of freedom above the cutoff, thereby drastically reducing the undesirable (or unphysical) sensitivity to short-distance physics.

V. THE hep PROCESS

In the notation of MSVKRB, the GT amplitude for the hep process is given in terms of the reduced matrix elements $\overline{L_1}(q;A)$ and $\overline{E_1}(q;A)$. Since these matrix elements are related to each other as $\overline{E_1}(q;A)\simeq\sqrt{2}\,\overline{L_1}(q;A)$, with the exact equality holding at $q=0$, we consider here only one of them $\overline{L_1}(q;A)$. For the three exemplary values of Λ, Table III gives the corresponding values of $\overline{L_1}(q;A)$ at $q\equiv|\boldsymbol{q}|=19.2$ MeV and zero c.m. energy; for convenience, the values of $\hat{d}^R$ in Eq. (24) are also listed. We see from the table that the variation of the two-body GT amplitude (row labeled "2B total") is ~10 % for the range of Λ under study. It is also noteworthy that the variation of the 2B amplitude as a function of Λ is reduced by a factor of ~7 by introducing the $\hat{d}^R$ term contributions; compare the fifth and seventh rows [labeled "2B (without $\hat{d}^R$)" and "2B total," respectively] in Table III. Although the Λ dependence in the total GT amplitude ($\overline{L_1}$ in the third row) is more pronounced due to the drastic cancellation between the 1B and 2B terms, this amplified Λ dependence still lies within acceptable levels for the purpose of analyzing the Super-Kamiokande data [48].

Table IV shows the contribution to the S factor, at zero c.m. energy, from each initial channel. For comparison we also give the results of MSVKRB for the AV18/UIX interaction. It is noteworthy that for all the channels other than $^3S_1$, the Λ dependence is very small ($\lesssim2\%$). The $^3S_1$ channel is the most sensitive to short-distance physics because the extraordinary suppression of the one-body GT contribution makes more pronounced the chiral-non-protected nature of the GT transition. In fact, the sensitivity of the $^3S_1$ channel to short-distance physics would be larger if the contribution of the A^0 term, which is rather sizable here despite its generic $1/m$ suppression, were omitted. It is therefore reassuring that the chiral-filter mechanism allows reliable estimation

TABLE IV. Contributions to $S_{\rm hep}(0)$ (in 10^{-20} keV b) from individual initial channels calculated as functions of Λ. The last column gives the results obtained in MSVKRB.

Λ (MeV)	500	600	800	MSVKRB
$^1S_0$	0.02	0.02	0.02	0.02
$^3S_1$	7.00	6.37	4.30	6.38
$^3P_0$	0.67	0.66	0.66	0.82
$^1P_1$	0.85	0.88	0.91	1.00
$^3P_1$	0.34	0.34	0.34	0.30
$^3P_2$	1.06	1.06	1.06	0.97
Total	9.95	9.37	7.32	9.64

of the A^0 term in this channel as well (in addition to the P-wave channels), see Ref. [18].

Summarizing the results given in Table IV, we arrive at a prediction for the hep S factor [49]:

$$S_{\rm hep}(0)=(8.6\pm1.3)\times10^{-20}\ \text{keV b}, \tag{31}$$

where the "error" spans the range of the Λ dependence for $\Lambda=500$–800 MeV. This result should be compared to that obtained by MSVKRB [18], $S_{\rm hep}(0)=9.64\times10^{-20}$ keV b [50].

The latest analysis of the Super-Kamiokande data [48] gives an upper limit of the solar hep neutrino flux, $\Phi(\text{hep})^{\rm SK}<40\times10^3\ \text{cm}^{-2}\ \text{s}^{-1}$. The standard solar model [51] using the hep S factor of MSVKRB [18] predicts $\Phi(\text{hep})^{\rm SSM}=9.4\times10^3\ \text{cm}^{-2}\text{s}^{-1}$. The use of the central value of our estimate Eq. (31) of the hep S factor would slightly lower $\Phi(\text{hep})^{\rm SSM}$ but with the upper limit compatible with $\Phi(\text{hep})^{\rm SSM}$ in Ref. [51]. A significantly improved estimate of $S_{\rm hep}(0)$ in Eq. (31) is expected to be useful for further discussion of the solar hep problem.

To reduce the uncertainty in Eq. (31), we need to reduce the Λ dependence in the two-body GT term. According to a general tenet of EFT, the cutoff dependence should diminish as higher order terms get included. In fact, the somewhat rapid variation seen in $\hat{d}^R$ (Table III) and in the $^3S_1$ contribution to $S_{\rm hep}(0)$ (Table IV) as Λ approaches 800 MeV may be an indication that there is need for the explicit presence of the vector mesons (ρ and ω) with mass $m_V\lesssim\Lambda$. This possible insufficiency could be remedied to a certain extent by going to higher orders. A preliminary study [52] indicates that it is indeed possible to reduce the Λ dependence significantly by including N^{4}LO corrections. We expect that the higher order correction would make the result for $\Lambda=800$ MeV closer to those for $\Lambda=500$,600 MeV, bringing the EFT* results closer to what was obtained in MSVKRB. This possibility is taken into account in the error estimate given in Eq. (31).

VI. DISCUSSION

It is worth emphasizing that the above EFT* prediction for $\delta_{\rm 2B}$ for the pp process is in line with the latest SNPA results obtained in Ref. [27] (and mentioned earlier). There too, the short range behavior of the axial MEC was con-

strained by reproducing Γ^t_β. The inherent model dependence of such a procedure within the SNPA context was shown to be very weak simply because at small inter-particle separations, where MEC contributions are largest, the pair wave functions in different nuclei are similar in shape and differ only by a scale factor [53]. As a consequence, the ratios of GT and pp-capture matrix elements of different two-body current terms are nearly the same, and therefore a knowledge of their sum in the GT matrix element is sufficient to predict their sum in the pp-capture matrix element [27].

It seems informative to compare the hep reaction with radiative np capture. The polarization observables in $\vec{n}+\vec{p} \to d+\gamma$ are known to be sensitive to the isoscalar $M1$ matrix element $M1S$, and this amplitude has been extensively studied in EFT [24,54]. The similar features of the hep GT amplitude and $M1S$ are (i) the leading one-body contribution is suppressed by the symmetries of the wave functions; (ii) there is no soft-pion exchange contribution; (iii) nonetheless, short-range physics can be reliably subsumed into a single contact term. In the $\vec{n}\vec{p}$ case the strength of this term can be determined from the deuteron magnetic moment (for a given value of Λ). The calculation in Ref. [24] demonstrates that the Λ dependence in the contact term and that of the remaining terms compensate each other so that the total $M1S$ is stable against changes in Λ. This suggests that, if we go to higher orders, the coefficient of the contact term in question will be modified, with part of its strength shifted to higher order terms; however, the total physical amplitude will remain essentially unchanged. These features are quite similar to what we have found here for the hep GT amplitude.

We have derived here all the weak currents up to N^{4}LO (even though we have calculated the relevant nuclear matrix elements only up to N^{3}LO). As Table I indicates, loop contributions start at N^{4}LO. Loop corrections in the vector currents (both $\boldsymbol{V}$ and V^0) can be safely ignored, since even their leading single-particle terms are suppressed relative to the axial current. It turns out that the loop diagrams in $\boldsymbol{A}$ are all finite and hence need no regularization although there are finite counterterms that should be taken into account. On the other hand, the loop diagrams in A_0 do have divergences and need to be regularized. To derive the momentum space expressions for the currents given above, we have employed the dimensional regularization. This is not quite congruous with the cutoff regularization adopted in going from momentum to coordinate space. Meanwhile, using a cutoff regularization in evaluating loop graphs is a delicate matter, since that might endanger chiral symmetry; with the use of a cutoff regularization one might need chiral-symmetry-breaking counterterms in order to satisfy the Ward identities. We have not yet investigated whether the dimensional regularization as used here preserves chiral symmetry, and hence we cannot say at this point whether our coordinate space operators at N^{4}LO are fully consistent. However, this problem does not arise if we limit ourselves to N^{3}LO, for up to this order there are no loop contributions.

Evaluating the matrix element of the leading-order one-body operator in EFT with the use of realistic nuclear wave functions is analogous to fixing parameters in an EFT Lagrangian (at a given order) using empirical inputs [55]; the realistic wave functions in SNPA can be regarded as a theoretical input that fits certain sets of observables. In the present EFT* scheme, we take the view that the same realistic wave functions also provide a framework for reliably calculating (finite-range) many-body corrections to the leading-order one-body matrix element. The short-ranged part inherited from the integrated out degrees of freedom is renormalized by the $\hat{d}^R$ term. This way of handling ''short-range correlation'' is analogous to the derivation of Bogner *et al.* [4] of ''$V_{\text{low-}k}$'' based on renormalization-group theory (see also the work of Epelbaum *et al.* [56]). While our approach here is, in certain cases, not in strict accordance with the systematic power-counting scheme of EFT proper, one should expect that the severity of this potential shortcoming may very well vary from one case to another (see discussion in Ref. [57]). For the pp and hep amplitudes under consideration, the degree of Λ dependence exhibited by the numerical results does suggest that deviations from rigorous power counting cannot be too significative. Indeed, this type of ''resilience'' may also explain why the SNPA calculation in Ref. [18] gives a result very similar to the present one. It is true that the two-body terms in MSVKRB are not entirely in conformity with the chiral counting scheme we are using here; some terms corresponding to chiral orders higher than N^{3}LO are included, while some other terms which are N^{3}LO in EFT are missing (see Appendix A 3). Most importantly the $\hat{d}^R$ term — which plays a crucial role here — is omitted in MSVKRB although heavy-meson exchange graphs may account for some part of it. This formal problem, however, seems to be largely overcome by the fact that also in MSVKRB a parameter (the axial $N\Delta$ coupling strength) is adjusted to reproduce Γ^t_β.

Not unrelated to the above issue of power counting is the question of consistency of embedding ''realistic'' wave functions obtained from ''realistic'' potentials that are fitted *accurately* to experiments into an EFT framework with the currents obtained to a given order of chiral perturbation theory. It is a well-known fact that potentials that fit experiments are not necessarily unique. The nonuniqueness resides, however, in the short-range part of the potential, with the long-range part primarily governed by the pion exchange. Let us suppose that one can calculate potentials to a very high order in a consistent expansion (that is, consistent with symmetries, etc.). The structure of the potential would depend on various aspects of the calculation. For instance, although they all may fit equally well various experimental data such as, e.g., nucleon-nucleon scattering, different regularizations would lead to different potentials, the difference residing mainly in the short-range part. One might worry that this nonuniqueness would upset the basic premise of an EFT, rendering the predictions untrustworthy [58].

Another intricate issue, which is also connected to short-range physics, is the off-shell ambiguity. This problem should be absent in a formally consistent EFT. In EFT*, however, we insert the current operators derived from irreducible diagrams up to a given chiral order between phenomenological (albeit realistic) wave functions. Since the in-

serted current involves off-shell particles, there can in principle be terms other than those that have been included in our approach. While those additional terms that may be required to eliminate the off-shell dependence are expected to be of higher order than N^3LO, this issue warrants a further examination.

To answer the above question with full rigor, much more work is needed. However, partial and yet reasonably satisfactory answers can be obtained from this work. For chiral-filter protected processes, we have presented a clear argument that the above-mentioned ambiguity does not matter at the level of accuracy in question. The results listed in Table IV for the *P*-wave capture (to which the chiral-protected time component of the axial current contributes) demonstrate this point. The question of short-distance ambiguity arises only for chiral-unprotected processes such as the GT transition. As already explained, however, the $\hat{d}^R$ renormalization essentially removes this ambiguity. The point is that the physics of the degrees of freedom above the cutoff scale Λ gets lodged in the short-range $\hat{d}^R$ term. In fixing this term as a function of Λ via the experimental value of Γ^t_β, one is essentially incorporating the short-range correlations that render low-energy physics insensitive to short-distance physics.

As for the off-shell problem, we note that for processes involving a long-wavelength external current — such as the solar pp and hep reactions — the off-shell ambiguity should be small in our scheme where the short-range contribution has been correctly renormalized, so long as one uses high-quality phenomenological wave functions that accurately describe processes without the external current. The wave functions used here describe with high accuracy a rich ensemble of data available for the systems in question; they describe very well the three-nucleon scattering states, and furthermore, the n^3He elastic scattering cross section as well as the coherent scattering length calculated with these wave functions are in excellent agreement with the experiments. What is involved here seems to be a generic feature. A similar stabilizing mechanism is at work when Bogner *et al.* [4] arrive at a unique effective force $V_{\text{low-}k}$ by integrating out the high-energy/momentum components contained in various ''realistic'' potentials. Nuclear physics calculations done with this effective force [59] have much in common with the EFT* calculation described here. Furthermore, we remark that different off-shell properties reflect different choices of the field variables and that, for each choice, the LECs need to be readjusted. It is in principle possible to choose the field variables in such a manner that off-shell contributions become highly suppressed. We are essentially adopting this particular choice by using the forms of the transition operators described above and adjusting the corresponding LEC $\hat{d}^R$ to reproduce Γ^t_β.

A possible approach that is formally consistent with systematic power counting is the pionless EFT based on the power divergence subtraction (PDS) scheme [60] (for a recent review, see Ref. [61]), which has been applied to the pp fusion [62]. Due to the fact that this scheme also involves one unknown low-energy constant, PDS has not so far led to a definite prediction on the pp fusion rate. The problem is that this approach cannot be readily extended to systems with $A \geqslant 3$, in particular to electroweak transition amplitudes in these systems. What is lacking presently is a method to correlate in a unified framework the observables in different nuclei (different mass numbers). This limitation keeps one from exploiting the experimental data available for the $A \geqslant 3$ nuclei to fix unknown LEC. Apart from the basic problem of organizing chiral expansion for complex nuclei from ''first-principles,'' a plethora of parameters involved would present a major obstacle. (For recent efforts in this approach, see Refs. [61,63] and references given therein.) This difficulty is expected to be particularly pronounced for the hep reaction.

There has been a series of intensive studies by the Jülich Group to extend EFT calculations in the Weinberg scheme to systems with three or more nucleons [64]. The relationship between this approach and the phenomenological potential approach has been examined in great detail. This line of study, however, has been so far limited to nuclear observables that do *not* involve the electroweak currents. An extension of the formalism developed in Ref. [64] to electroweak transitions should be extremely useful.

ACKNOWLEDGMENTS

T.S.P. and K.K. thank S. Ando and F. Myhrer for discussions. M.R. is grateful for clarifying discussions with Gerry Brown on the notion of ''double decimation'' in nuclear structure theory. The work of T.S.P. and K.K. was supported in part by the U.S. National Science Foundation, Grant No. PHY-9900756 and No. INT-9730847. The work of R.S. was supported by DOE Contract No. DE-AC05-84ER40150, under which the Southeastern Universities Research Association (SURA) operates the Thomas Jefferson National Accelerator Facility. The work of D.P.M. is supported in part by KOSEF Grant No. 1999-2-111-005-5 and KSF Grant No. 2000-015-DP0072. M.R. acknowledges the hospitality of the Physics Departments of the Seoul National University and Yonsei University, where his work was partially supported by Brain Korea 21 in 2001. T.S.P. and K.K. would like to thank Korea Institute for Advanced Study for the hospitality accorded to them while part of this paper was being written. Some of the calculations were made possible by grants of computing time from the National Energy Research Supercomputer Center in Livermore.

APPENDIX A: GAMOW-TELLER OPERATORS

The aim of this and subsequent Appendixes is to provide some technical details that have been left out in the main text. The readers who are not interested in the details of our calculation can safely skip these Appendixes without missing the essential points of our results.

We decompose the axial current into n_B-body operators as

$$A^{\mu,a} = A^{\mu,a}_{1\text{B}} + A^{\mu,a}_{2\text{B}} + A^{\mu,a}_{3\text{B}} + \cdots$$

$$= \sum_l A^{\mu,a}_l + \sum_{l<m} A^{\mu,a}_{lm} + \sum_{l<m<n} A^{\mu,a}_{lmn} + \cdots, \tag{A1}$$

where (l, m, n) are particle indices. The one-body operator can be read from

$$\langle N(p')|A^{\mu,a}(x=0)|N(p)\rangle = -\overline{u}(p')\left[G_A(q^2)\gamma^\mu\gamma_5 - \frac{G_P(q^2)}{2m_N}q^\mu\gamma_5\right]\frac{\tau^a}{2}u(p), \tag{A2}$$

where $u(p)$ is a four-component Dirac spinor of momentum p, and $q^\mu=(p-p')^\mu$ is the momentum carried by the lepton pair. $G_A(q^2)$ and $G_P(q^2)$ are the axial and induced pseudoscalar form factors, respectively. Note that $q^\mu=\mathcal{O}(Q^2/m_N)$, while $\boldsymbol{p}=\mathcal{O}(Q)$ and $\boldsymbol{p}\,'=\mathcal{O}(Q)$. Thus, up to N^{3}LO, it is sufficient to consider the form factors at $q^2=0$. Furthermore $\overline{u}(p')q^\mu\gamma_5 u(p)$ attached to the G_P term is of $\mathcal{O}(Q^4/\Lambda_\chi^3)$, which we neglect throughout this work [65]. In getting the nonrelativistic operators from the above relativistic form factors, we should also take into account the wave function normalization. The resulting one-body operator up to $\mathcal{O}(Q^3)$ then reads

$$\boldsymbol{A}_l^a = -\frac{\tau_l^a}{2}g_A e^{-i\boldsymbol{r}_l\cdot\boldsymbol{q}}\left[\boldsymbol{\sigma}_l + \frac{\overline{\boldsymbol{p}_l}\boldsymbol{\sigma}_l\cdot\overline{\boldsymbol{p}_l} - \boldsymbol{\sigma}_l\overline{\boldsymbol{p}_l^2}}{2m_N^2} + \frac{i\boldsymbol{q}\times\boldsymbol{p}_l}{4m_N^2} + \mathcal{O}\left(\frac{Q^4}{m_N^4}\right)\right]. \tag{A3}$$

This expression has appeared in Eq. (17). In the following subsections, we derive all the two-body GT operators up to N^{4}LO and leading three-body GT operators.

1. Two-body GT

There are no two-body GT diagrams that involve only $\nu_i=0$ vertices, because the $\mathcal{A}^{i,a}\pi NN$ vertex is kinematically suppressed, and there is no four-fermion contact contribution at LO ($\nu_i=0$). As a consequence, the two-body GT operator starts at $\nu=3$. The two-body GT operator at threshold ($q^\mu\to 0$) was given up to N^{3}LO in Ref. [36]. We extend here that analysis to include all contributions up to N^{4}LO. To this end, it is useful to decompose $\boldsymbol{A}_{lm}^a$ as

$$\boldsymbol{A}_{lm}^a = \boldsymbol{A}_{lm}^a(1\pi) + \boldsymbol{A}_{lm}^a(2\pi), \tag{A4}$$

where $\boldsymbol{A}_{lm}^a(1\pi)$ represents the contributions of the one-pion pole part and $\boldsymbol{A}_{lm}^a(2\pi)$ stands for the remaining short-ranged part. Generic diagrams for $\boldsymbol{A}_{lm}^a(1\pi)$ and $\boldsymbol{A}_{lm}^a(2\pi)$ are shown in Fig. 1.

We now list all the two-body GT operators belonging to $\nu=3$ and $\nu=4$.

$\nu=3$. This contribution comes from tree graphs (one-pion-exchange and contact) with a $\nu_i=1$ vertex. The resulting GT operators, given in Ref. [36], are of the form

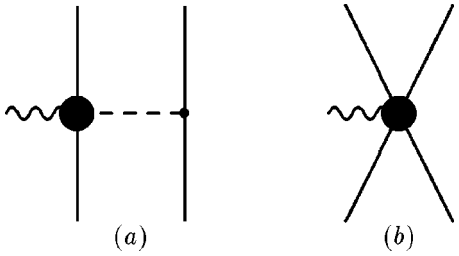

FIG. 1. A one-pion pole diagram (a) responsible for $\boldsymbol{A}_{lm}^a(1\pi)$, and a short-range contribution diagram (b) responsible for $\boldsymbol{A}_{lm}^a(2\pi)$. The solid circles include counterterm insertions and (one-particle irreducible) loop corrections. The wiggly line stands for the external field (current) and the dashed line for the pion. One-loop corrections of the relevant orders for the pion propagator and the πNN vertex need to be included.

$$\boldsymbol{A}_{12}^{a;\nu3}(1\pi) = \frac{g_A}{2m_N f_\pi^2}\left[\frac{i}{2}(\vec{\tau}_1\times\vec{\tau}_2)^a\overline{\boldsymbol{p}_1} + 2\hat{c}_3\tau_2^a\boldsymbol{k}_2 + \left(\hat{c}_4+\frac{1}{4}\right)(\vec{\tau}_1\times\vec{\tau}_2)^a\boldsymbol{\sigma}_1\times\boldsymbol{k}_2 + \frac{1+c_6}{4}(\vec{\tau}_1\times\vec{\tau}_2)^a\boldsymbol{\sigma}_1\times\boldsymbol{q}\right]\frac{\boldsymbol{\sigma}_2\cdot\boldsymbol{k}_2}{\boldsymbol{k}_2^2+m_\pi^2} + (1\leftrightarrow 2), \tag{A5}$$

$$\boldsymbol{A}_{12}^{a;\nu3}(2\pi) = \frac{g_A}{m_N f_\pi^2}[\hat{d}_1(\tau_1^a\boldsymbol{\sigma}_1+\tau_2^a\boldsymbol{\sigma}_2) + \hat{d}_2(\vec{\tau}_1\times\vec{\tau}_2)^a\boldsymbol{\sigma}_1\times\boldsymbol{\sigma}_2], \tag{A6}$$

where $\boldsymbol{k}_l\equiv\boldsymbol{p}_l'-\boldsymbol{p}_l$. Although there are two unknown parameters, $\hat{d}_1$ and $\hat{d}_2$, it turns out that the Fermi-Dirac statistics effectively reduces the number of unknowns to one. We will come back to this important point later.

$\nu=4$. Tree graphs with $\Sigma_i\nu_i=2$ and one-loop graphs with $\Sigma_i\nu_i=0$ enter at this order. Since there is no πNN vertex with $\nu_i=1$, a $\nu=4$ tree graph should have either $\boldsymbol{A}(NN)^2$ or $\boldsymbol{A}\pi NN$ vertex with $\nu_i=2$. We can, however, exclude either possibility. The absence of $\boldsymbol{A}\pi NN$ vertex at $\nu_i=2$ can be ascertained by consulting a complete list of terms that appear in the N^{2}LO Lagrangian given in Ref. [66]. As for the $\nu_i=2$ $\boldsymbol{A}(NN)^2$ vertex for the two-nucleon sector, a complete list is not available yet. We therefore resort to parity selection rules. Our vertex must have one Δ_μ and one D_μ involving four nucleon fields. These operators should not be contracted with the four-velocity v^μ, for otherwise the actual chiral index would acquire an extra power of Q. We can easily show, however, that it is impossible to construct a parity-even Lorentz scalar with one Δ_μ, one D_μ and arbitrary numbers of S^μ and $\epsilon^{\mu\nu\alpha\beta}$. Introducing an operator of the $\partial_\mu A_\nu-\partial_\nu A_\mu$ type instead of Δ_μ and D_μ does not help either. These observations lead us to conclude that no divergences occur in the relevant loops and, more importantly, that no new parameters appear at $\nu=4$.

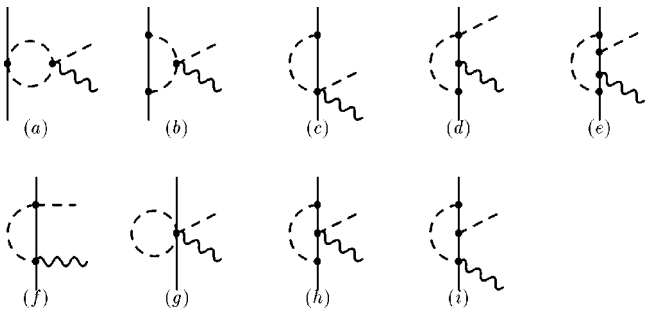

FIG. 2. One loop diagrams that contribute to the $\mathcal{A}^\mu \pi NN$ vertex. Only the first five diagrams (a)–(e) contribute to $\boldsymbol{A}$.

The one-pion-exchange contribution can be read off from one-loop corrections to the $\Gamma^{\mu,ab}_{\mathcal{A}\pi}$ vertex; the relevant diagrams are shown in Fig. 2. We note that only the first five diagrams (a)–(e) contribute to $\boldsymbol{A}$. Using the expressions given in Ref. [15], where all the one-loop diagrams have been calculated, we find

$$\begin{aligned}\boldsymbol{A}^{a;\nu 4}_{12}(1\pi) = &-\frac{g_A^3}{32\pi f_\pi^4}\Bigg[(\vec{\tau}_1\times\vec{\tau}_2)^a\Bigg(\boldsymbol{\sigma}_1\times(\boldsymbol{k}_2+\boldsymbol{q})D_1(k_1)\\ &+\frac{g_A^2}{8}\boldsymbol{\sigma}_1\times\boldsymbol{k}_2\; m_\pi\Bigg)-\tau_2^a\Bigg((\boldsymbol{q}+3\boldsymbol{k}_2)\Bigg[D_1(k_1)\\ &+\frac{1}{3}\boldsymbol{k}_1^2 D_2(k_1)\Bigg]+\frac{9g_A^2}{8}\boldsymbol{k}_2\; m_\pi\Bigg)\Bigg]\times\frac{\boldsymbol{\sigma}_2\cdot\boldsymbol{k}_2}{m_\pi^2+\boldsymbol{k}_2^2}\\ &+(1\leftrightarrow 2),\end{aligned} \tag{A7}$$

where $k_l=|\boldsymbol{k}_l|$ $(l=1,2)$, and $D_i(k)$'s are defined as

$$D_1(k)=\int_0^1 dz M_{zk},$$

$$D_2(k)=\int_0^1 dz\;\frac{z\bar{z}}{M_{zk}},$$

$$\begin{aligned}D_3(k)&=\int_0^1 dz\;\left(-\frac{z\bar{z}\boldsymbol{k}^2}{M_{zk}}-5M_{zk}\right)\\ &=4\int_0^1 dz\;\left(-\frac{3}{2}M_{zk}+\frac{m_\pi^2}{4M_{zk}}\right),\end{aligned}$$

$$\begin{aligned}D_4(k)&=\int_0^1 dz\left(-\frac{(z\bar{z})^2\boldsymbol{k}^2}{M_{zk}^3}+7\frac{z\bar{z}}{M_{zk}}-\frac{1}{M_{zk}}\right)\\ &=4\int_0^1 dz\;\left[\frac{z\bar{z}}{2M_{zk}}+\frac{z\bar{z}m_\pi^2}{4M_{zk}^3}-\left(\frac{1}{4}-z\bar{z}\right)\frac{1}{M_{zk}}\right],\end{aligned}$$

$$D_5(k)=\int_0^1 dz\;\frac{1}{M_{zk}},$$

$$D_6(k)=\int_0^1 dz\;\left(\frac{1}{4}-z\bar{z}\right)\frac{1}{M_{zk}}. \tag{A8}$$

Here $k\equiv|\boldsymbol{k}|$, $\bar{z}\equiv 1-z$, and $M_{zk}\equiv\sqrt{m_\pi^2+z\bar{z}\,\boldsymbol{k}^2}$.

The integrations over z can be done analytically, resulting in

$$\begin{aligned}D_1(k)&=\frac{m_\pi}{2}+\frac{4m_\pi^2+k^2}{4k}\Theta_k,\\ D_2(k)&=\frac{m_\pi}{2k^2}-\frac{4m_\pi^2-k^2}{4k^3}\Theta_k,\\ D_3(k)&=-3m_\pi-\frac{8m_\pi^2+3k^2}{2k}\Theta_k,\\ D_4(k)&=\frac{1}{2k^3}\left[\frac{2m_\pi k(8m_\pi^2+3k^2)}{4m_\pi^2+k^2}-(8m_\pi^2+k^2)\Theta_k\right],\\ D_5(k)&=\frac{2}{k}\Theta_k,\\ D_6(k)&=-\frac{m_\pi k}{2k^3}+\frac{4m_\pi^2+k^2}{4k^3}\Theta_k,\end{aligned} \tag{A9}$$

where $k\equiv|\boldsymbol{k}|$ and

$$\Theta_k\equiv\tan^{-1}\frac{k}{2m_\pi} \tag{A10}$$

with $-\pi/2<\Theta_k<\pi/2$.

Note that the one-pion-pole contributions can be absorbed into $\boldsymbol{A}^{a;\nu 3}_{lm}(1\pi)$ [given in Eq. (A5)] by renormalizing $\hat{c}_3$ and $\hat{c}_4$,

$$\begin{aligned}\hat{c}_3\rightarrow\hat{c}_3^R&\equiv\hat{c}_3+\frac{m_N g_A^2}{32\pi f_\pi^2}\left[\tilde{D}_{1\pi}+\frac{9g_A^2}{8}m_\pi\right]\\ &\simeq\hat{c}_3+1.0334,\\ \hat{c}_4\rightarrow\hat{c}_4^R&\equiv\hat{c}_4-\frac{m_N g_A^2}{32\pi f_\pi^2}\left[2D_{1\pi}+\frac{g_A^2}{8}m_\pi\right]\\ &\simeq\hat{c}_4-0.4821,\end{aligned} \tag{A11}$$

where

$$\begin{aligned}D_{1\pi}&\equiv D_1(k)\big|_{k^2=-m_\pi^2}=\frac{m_\pi}{4}\left[2+3\tanh^{-1}\frac{1}{2}\right],\\ \tilde{D}_{1\pi}&\equiv 3D_1(k)+k^2D_2(k)\big|_{k^2=-m_\pi^2}\\ &=m_\pi\left[2+\tanh^{-1}\frac{1}{2}\right].\end{aligned} \tag{A12}$$

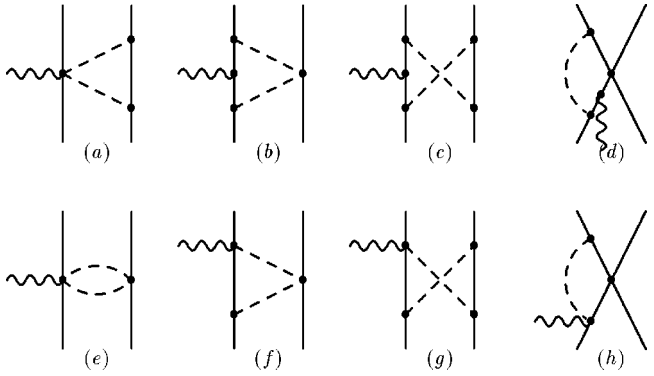

FIG. 3. One loop diagrams for the $\boldsymbol{A}_{lm}^{a:\nu 4}(2\pi)$: the first four diagrams (a)–(d) contribute to the space part of the axial-vector (GT) and the remaining diagrams (f)–(h) to the axial-charge current. The graph (e) vanishes.

For the two-pion contribution $\boldsymbol{A}_{lm}^{a:\nu 4}(2\pi)$, the relevant one-loop graphs are shown in Fig. 3. Among the diagrams in the figure, only the first four graphs (a)–(d), can contribute to the GT operator; (e) is identically zero due to isospin symmetry, and the remaining graphs, (f)–(h), contribute only to A^0.

As mentioned, the four diagrams (a)–(d) are all ultraviolet finite. The first three graphs give

$$\boldsymbol{A}_{12}^{a}(2\pi{:}a)=-\frac{g_A^3}{64\pi f_\pi^4}\boldsymbol{\sigma}_1\tau_1^a[3D_1(k_2)+\boldsymbol{k}_2^2D_2(k_2)] +(1\leftrightarrow 2),$$

$$\boldsymbol{A}_{12}^{a}(2\pi{:}b)=-\frac{g_A^3}{128\pi f_\pi^4}\tau_2^a[\boldsymbol{\sigma}_1D_1(k_2)-(2\boldsymbol{k}_2\boldsymbol{\sigma}_1\cdot\boldsymbol{k}_2 -\boldsymbol{\sigma}_1\boldsymbol{k}_2^2)D_2(k_2)]+(1\leftrightarrow 2),$$

$$\boldsymbol{A}_{12}^{a}(2\pi{:}c)=-\frac{g_A^5}{1024\pi f_\pi^4}(\tau_1^a+2\tau_2^a)[\boldsymbol{\sigma}_1D_3(k_2)+(2\boldsymbol{k}_2\boldsymbol{\sigma}_1\cdot\boldsymbol{k}_2 -\boldsymbol{\sigma}_1\boldsymbol{k}_2^2)D_4(k_2)+(\boldsymbol{\sigma}_2\boldsymbol{k}_2^2-\boldsymbol{k}_2\boldsymbol{\sigma}_2\cdot\boldsymbol{k}_2)D_5(k_2)] +(1\leftrightarrow 2) \tag{A13}$$

while the fourth diagram (d) gives

$$\boldsymbol{A}_{12}^{a}(2\pi{:}d)=-\frac{g_A^3m_\pi}{64\pi f_\pi^2}\sum_A\ \tau_1^b\boldsymbol{\sigma}_1^j\{C_A\Gamma_A\Gamma_A,\tau_1^a\boldsymbol{\sigma}_1\}\tau_1^b\boldsymbol{\sigma}_1^j +(1\leftrightarrow 2). \tag{A14}$$

The summation here is taken over all possible combinations of spin-isospin operators (with no derivatives) that figure in the nucleon-nucleon interactions. Using a generic expression

$$\sum_A\ C_A\Gamma_A\Gamma_A=X_1+\boldsymbol{\sigma}_1\cdot\boldsymbol{\sigma}_2X_{\boldsymbol{\sigma}}+\vec{\tau}_1\cdot\vec{\tau}_2X_\tau+\boldsymbol{\sigma}_1\cdot\boldsymbol{\sigma}_2\vec{\tau}_1\cdot\vec{\tau}_2X_{\boldsymbol{\sigma}\tau}, \tag{A15}$$

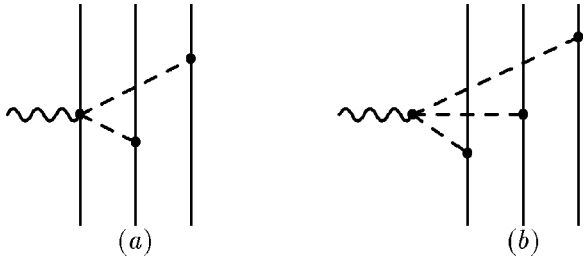

FIG. 4. Diagrams for the three-body GT operator. All other diagrams are higher order than N^{4}LO except for the crossed diagrams of (a) — crossed with respect to the particle indices.

where X_1, $X_{\boldsymbol{\sigma}}$, X_τ, $X_{\boldsymbol{\sigma}\tau}$ are constants that characterize the LO short-range nuclear forces, we can write

$$\boldsymbol{A}_{12}^{a}(2\pi{:}d)=-\frac{g_A^3m_\pi}{32\pi f_\pi^2}[(-3X_1+9X_{\boldsymbol{\sigma}\tau})(\tau_1^a\boldsymbol{\sigma}_1+\tau_2^a\boldsymbol{\sigma}_2) +(-2X_{\boldsymbol{\sigma}\tau})(\vec{\tau}_1\times\vec{\tau}_2)^a(\boldsymbol{\sigma}_1\times\boldsymbol{\sigma}_2) +(9X_{\boldsymbol{\sigma}}-3X_\tau)(\tau_1^a\boldsymbol{\sigma}_2+\tau_2^a\boldsymbol{\sigma}_1)]. \tag{A16}$$

We demonstrate below that X's can all be absorbed into the parameters $\hat{d}$'s.

2. Three-body GT

The three-body GT operators up to N^{4}LO come from the two diagrams given in Fig. 4. They contain only $\nu_i=0$ vertices, and their contributions read

$$\boldsymbol{A}_{123}^{a}=-\sum_{\text{cycle}(123)}\ \frac{g_A^3}{16f_\pi^4}(2\tau_1^a\ \ \vec{\tau}_2\cdot\vec{\tau}_3-\tau_2^a\ \ \vec{\tau}_3\cdot\vec{\tau}_1-\tau_3^a\ \ \vec{\tau}_1\cdot\vec{\tau}_2) \times\left(\boldsymbol{\sigma}_1-\frac{4}{3}\frac{\boldsymbol{k}_1\boldsymbol{\sigma}_1\cdot\boldsymbol{k}_1}{\boldsymbol{k}_1^2+m_\pi^2}\right)\frac{\boldsymbol{\sigma}_2\cdot\boldsymbol{k}_2}{\boldsymbol{k}_2^2+m_\pi^2}\frac{\boldsymbol{\sigma}_3\cdot\boldsymbol{k}_3}{\boldsymbol{k}_3^2+m_\pi^2}, \tag{A17}$$

where

$$\sum_{\text{cycle}(lmn)}\ f_{lmn}\equiv f_{lmn}+f_{mnl}+f_{nlm}. \tag{A18}$$

3. Comparison with SNPA exchange currents

The meson-exchange currents in SNPA [67,68] are based on one-boson exchange diagrams involving those bosons which are responsible for the phenomenological nuclear forces in the context of one-boson-exchange models. This framework does not have direct contact with chiral counting. We give here a detailed comparison between the transition operators used in SNPA and those dictated by χPT. Among the most elaborate SNPA operators are the ones used in CRSW91 [16]; these operators were derived by Towner [68] based on a phenomenological Lagrangian [69] which satisfies CVC, PCAC and current algebra. We consider the SNPA operators used in CRSW91 as a representative. It will turn

out that there are substantial differences between the SNPA and χPT operators in both the long-range and short-range parts.

In CRSW91 the heavy particles ρ and Δ are treated as explicit degrees of freedom [70]. To examine the roles of these heavy particles in the context of the present comparison, we divide the two-body currents in CRSW91 into two families:

$$\boldsymbol{A}^a = \boldsymbol{A}^a_{\rm I} + \boldsymbol{A}^a_{\rm II} \tag{A19}$$

$$\equiv [\boldsymbol{A}^a(\Delta\pi) + \boldsymbol{A}^a(\pi\rho) + \boldsymbol{A}^a(\pi S)] + [\boldsymbol{A}^a(\Delta\rho) + \boldsymbol{A}^a(\rho S)], \tag{A20}$$

where the "S" stands for "seagull." $\boldsymbol{A}^a_{\rm I}$ and $\boldsymbol{A}^a_{\rm II}$ can be associated, respectively, with $\boldsymbol{A}^a_{lm}(1\pi)$ and $\boldsymbol{A}^a_{lm}(2\pi)$ in Eq. (A4). The expression for $\boldsymbol{A}^a_{\rm I}$ is [71]

$$\begin{aligned}\boldsymbol{A}^a_{\rm I} = \frac{g_A}{2m_N f_\pi^2}\Bigg\{ & -\frac{4}{25} g_A^2 I_1 \frac{m_N}{m_\Delta - m_N} \mathcal{R}^2_\pi(\boldsymbol{k}_2) \\ & \times [4\tau_2^a \boldsymbol{k}_2 - (\vec{\tau}_1 \times \vec{\tau}_2)^a \boldsymbol{\sigma}_1 \times \boldsymbol{k}_2] \\ & - \frac{I_2}{4} \mathcal{R}_\rho(\boldsymbol{k}_1)\mathcal{R}_\pi(\boldsymbol{k}_2) \frac{m_\rho^2}{m_\rho^2 + \boldsymbol{k}_1^2} \\ & \times (\vec{\tau}_1 \times \vec{\tau}_2)^a [(1+\kappa)\boldsymbol{\sigma}_1 \times \boldsymbol{k}_1 - 2i\overline{\boldsymbol{p}_1}] \\ & + \frac{I_1}{4} g_A^2 \mathcal{R}^2_\pi(\boldsymbol{k}_2) [(\vec{\tau}_1 \times \vec{\tau}_2)^a \boldsymbol{\sigma}_1 \times \boldsymbol{k}_2 \\ & - \tau_2^a(-\boldsymbol{q} + 2i\boldsymbol{\sigma}_1 \times \overline{\boldsymbol{p}_1})] \Bigg\} \frac{\boldsymbol{\sigma}_2 \cdot \boldsymbol{k}_2}{m_\pi^2 + \boldsymbol{k}_2^2} + (1 \leftrightarrow 2)\end{aligned} \tag{A21}$$

with

$$\mathcal{R}_\pi(\boldsymbol{k}) \equiv \frac{\Lambda_\pi^2 - m_\pi^2}{\Lambda_\pi^2 + \boldsymbol{k}^2}, \quad \mathcal{R}_\rho(\boldsymbol{k}) \equiv \frac{\Lambda_\rho^2 - m_\rho^2}{\Lambda_\rho^2 + \boldsymbol{k}^2}, \tag{A22}$$

where $m_\Delta \simeq 1232$MeV, $\kappa \simeq 6.6$, and $g_\rho \simeq 2.50$ is the ρNN coupling constant; Λ_π (Λ_ρ) is a cutoff parameter characterizing the πNN (ρNN) coupling form factor. We have defined I_1 and I_2 by

$$I_1 \equiv \frac{4 f_\pi^2 f_{\pi NN}^2}{g_A^2 m_\pi^2} = \frac{f_{\pi NN}^2}{m_\pi^2} \cdot \left(\frac{g_A^2}{4 f_\pi^2} \right)^{-1}, \quad I_2 \equiv \frac{8 g_\rho^2 f_\pi^2}{m_\rho^2}. \tag{A23}$$

We note that $I_1 = 1$ if we assume the Goldberger-Treiman relation, and $I_2 = 1$ if the KSRF relation holds [72]. The above equation should be compared with $\boldsymbol{A}^{a;\nu 3}_{lm}(1\pi)$ in Eq. (A6). A little exercise shows that, while the currents $\boldsymbol{A}(\pi\Delta)$ and $\boldsymbol{A}(\pi\rho)$ can be related to certain currents in χPT, $\boldsymbol{A}(\pi S)$ has no χPT counterpart to the order considered here. A possible explanation for the occurrence of this "extra" term in SNPA is that $\boldsymbol{A}(\pi S)$ arises as a "recoil" term associated with the use of the pseudoscalar coupling. A χPT analog of $\boldsymbol{A}(\pi S)$ would be a $1/m_N$ term, but this term should be substantially suppressed; hence a term such as $\boldsymbol{A}(\pi S)$ should be absent in chirally invariant theory. Comparison of the coefficients of $(\vec{\tau}_1 \times \vec{\tau}_2)^a \overline{\boldsymbol{p}_1}$, $\tau_2^a \boldsymbol{k}_2$, $(\vec{\tau}_1 \times \vec{\tau}_2)^a \boldsymbol{\sigma}_1 \times \boldsymbol{k}_2$, and $(\vec{\tau}_1 \times \vec{\tau}_2)^a \boldsymbol{\sigma}_1 \times \boldsymbol{q}$ leads to the following correspondence between χPT (left-hand side) and CRSW91 (right-hand side):

$$1 \leftrightarrow I_2 \mathcal{R}_\rho(\boldsymbol{k}_1)\mathcal{R}_\pi(\boldsymbol{k}_2) \frac{m_\rho^2}{m_\rho^2 + \boldsymbol{k}_1^2}, \tag{A24}$$

$$\hat{c}_3 \leftrightarrow -\frac{8}{25} g_A^2 I_1 \frac{m_N}{m_\Delta - m_N} \mathcal{R}^2_\pi(\boldsymbol{k}_j), \tag{A25}$$

$$\hat{c}_4 + \frac{1}{4} \leftrightarrow \frac{4}{25} g_A^2 I_1 \frac{m_N}{m_\Delta - m_N} \mathcal{R}^2_\pi(\boldsymbol{k}_j) + I_2 \mathcal{R}_\rho(\boldsymbol{k}_1)\mathcal{R}_\pi(\boldsymbol{k}_2) \frac{m_\rho^2}{m_\rho^2 + \boldsymbol{k}_1^2} \frac{1+\kappa}{4}, \tag{A26}$$

$$1 + c_6 \leftrightarrow I_2 \mathcal{R}_\rho(\boldsymbol{k}_1)\mathcal{R}_\pi(\boldsymbol{k}_2) \frac{m_\rho^2}{m_\rho^2 + \boldsymbol{k}_1^2} \ (1+\kappa). \tag{A27}$$

The presence of the momentum-dependence in $\mathcal{R}$'s and the ρ-meson propagator prevents us from going beyond this correspondence. To proceed, however, we may consider the approximation

$$1 \approx I_2 \mathcal{R}_\rho(\boldsymbol{k}_1)\mathcal{R}_\pi(\boldsymbol{k}_2) \frac{m_\rho^2}{m_\rho^2 + \boldsymbol{k}_1^2} \approx I_1 \mathcal{R}^2_\pi(\boldsymbol{k}_j). \tag{A28}$$

We then find

$$\hat{c}_3^{\rm CRSW} = -\frac{8}{25} g_A^2 \frac{m_N}{m_\Delta - m_N} \simeq -1.633, \tag{A29}$$

$$\hat{c}_4^{\rm CRSW} = -\frac{1}{2}\hat{c}_3^{\rm CRSW} + \frac{\kappa}{4} \simeq 2.467, \tag{A30}$$

$$c_6^{\rm CRSW} = \kappa \simeq 6.6. \tag{A31}$$

It is informative to compare these values of $\hat{c}$'s with those obtained in a resonance-exchange saturation analysis by Bernard, Kaiser, and Meißner (BKM) [30]. We note that the two approaches give very different results for the Δ-resonance contributions. CRSW91 used the quark model value for the ratio $g_{AN\Delta}/g_{\pi N\Delta}$, the accuracy of which is rather difficult to assess. Meanwhile, the resonance-saturation calculation suffers from ambiguity related to the so-called off-shell parameter Z. Considering these uncertainties, it is perhaps not too surprising that BKM's estimate of the Δ contribution to $\hat{c}_3$, $|\hat{c}_3^\Delta| = 3.59$, is 2.2 times larger than the estimate in CRSW91. We also note that, while CRSW91 only includes the Δ and ρ-meson contributions, BKM's calculation con-

tains the contributions from scalar-meson and Roper exchanges as well. According to BMK,

$$\hat{c}_3^{\Delta}+\hat{c}_3^{\rm scalar}+\hat{c}_3^{\rm Roper}=-3.59-1.31-0.06=-4.96,$$

$$\hat{c}_4^{\Delta}+\hat{c}_4^{\rho}+\hat{c}_4^{\rm Roper}=1.80+1.53+0.11=3.44. \quad \text{(A32)}$$

Thus the contributions of the scalar-meson exchange are substantial. What is significant for our calculation is the fact that the coefficients c's can be extracted directly from the πN scattering data [30,66]. The most recent analysis [66] gives

$$\hat{c}_3=(-5.58\pm 0.08,\ -5.49\pm 0.01,\ -5.82\pm 0.08),$$

$$\hat{c}_4=(3.26\pm 0.05,\ 3.29\pm 0.01,\ 3.30\pm 0.04). \quad \text{(A33)}$$

These values are in reasonable agreement with those obtained in the resonance saturation approach. We should note, however, that the results in Eq. (A33) belong to an N^{4}LO calculation wherein $\Delta(1232)$ as well as other massive degrees of freedom have been integrated out. The explicit inclusion of $\Delta(1232)$ would modify the values of $\hat{c}$'s, because the Δ contribution to the $\hat{c}$'s should now be excluded. We also should pay attention to a similar modification of the LECs as we move from N^{4}LO to N^{3}LO. Although the difference between $\hat{c}$'s obtained in an N^{3}LO calculation and those obtained in N^{4}LO are of order of Q^4 and hence can in principle be neglected in an N^{3}LO calculation, it is more natural and safer to use in our present calculation the values obtained in an N^{3}LO analysis [30],

$$\text{N}^3\text{LO:}\quad \hat{c}_3=-4.96\pm 0.23,$$

$$\hat{c}_4=3.40\pm 0.09. \quad \text{(A34)}$$

The precise value of c_6 is unimportant in the present context, since it is suppressed by the kinematic factor $|\boldsymbol{q}|$. In any event, the results of BMK and CRSW91 are close to each other, $c_6\simeq 5.83$.

We now discuss the short-ranged currents $\boldsymbol{A}_{\rm II}^a=\boldsymbol{A}(\rho\Delta)+\boldsymbol{A}(\rho S)$. According to CRSW91, the dominant term in $\boldsymbol{A}_{\rm II}^a$ is of the form

$$\begin{aligned}\boldsymbol{A}^a(\rho\Delta)=&\frac{g_A}{2m_N f_\pi^2}I_2\frac{(1+\kappa)^2}{50m_N(m_\Delta-m_N)}\mathcal{R}_\rho^2(\boldsymbol{k}_2)\frac{m_\rho^2}{m_\rho^2+\boldsymbol{k}_2^2}\\&\times[4\tau_2^a(\boldsymbol{\sigma}_2\times\boldsymbol{k}_2)\times\boldsymbol{k}_2-(\vec{\tau}_1\times\vec{\tau}_2)^a\boldsymbol{\sigma}_1\\&\times[(\boldsymbol{\sigma}_2\times\boldsymbol{k}_2)\times\boldsymbol{k}_2]]+(1\leftrightarrow 2). \quad \text{(A35)}\end{aligned}$$

It should be noted, however, that this term belongs to N^{5}LO in chiral counting, and therefore its inclusion in CRSW91 constitutes a deviation from χPT. Although a particular N^{5}LO term may give an appreciable contribution (see below), there are many terms of the same order, including multiloop diagrams, and in general there should be a substantial cancellation among these terms to make the net N^{5}LO contribution small, as dictated by chiral symmetry. Thus, there are important differences between $\boldsymbol{A}_{\rm II}^a$ of CRSW91 and $\boldsymbol{A}(2\pi)$ derived in χPT.

APPENDIX B: AXIAL CHARGE OPERATORS

As stressed in the main text, the axial charge operators are chiral-protected. Since the axial-charge operators up to $\mathcal{O}(Q^4)$ have already been described in detail in Ref. [15], we only briefly recapitulate what is directly relevant to the present work. The leading one-body A^0 operator is kinematically suppressed because of the γ_5 matrix. Correspondingly, in χPT, the A^0 operator at order $\mathcal{O}(Q^1)$ appears as a $1/m_N$ term. The leading correction to the one-body axial-charge operator comes from the soft one-pion-exchange, which is of $\mathcal{O}(Q^2)$. Loop contributions start at $\mathcal{O}(Q^4)$, and hence the ratio of the loop contribution to the tree diagram two-body contribution is $\mathcal{O}(Q^2)$. Finally, there is no three-body contribution up to $\mathcal{O}(Q^4)$.

The one-body axial-charge operator at threshold is given by

$$A_l^{0,a}=-\frac{\tau_l^a}{2}g_A\left[\frac{\boldsymbol{\sigma}_l\cdot\overline{\boldsymbol{p}_l}}{m_N}+\mathcal{O}\left(\frac{\boldsymbol{q}^2}{m_N^2}\right)\right], \quad \text{(B1)}$$

which is $\mathcal{O}(Q^1)$. We note that there is no relativistic correction of $\mathcal{O}(\boldsymbol{q})$ to the one-body axial charge; this aspect is in sharp contrast to the GT operator.

The two-body A^0 current appears at $\mathcal{O}(Q^2)$ (tree diagram) and at $\mathcal{O}(Q^4)$ (loop diagrams):

$$A_{12}^{0,a}=-\frac{g_A}{4f_\pi^2}[\mathcal{T}^{a(\rm I)}\mathcal{W}^{(\rm I)}+\mathcal{T}^{a(\rm II)}\mathcal{W}^{(\rm II)}], \quad \text{(B2)}$$

where

$$\mathcal{T}^{a(\rm I)}=i(\vec{\tau}_1\times\vec{\tau}_2)^a\boldsymbol{k}\cdot(\boldsymbol{\sigma}_1+\boldsymbol{\sigma}_2), \quad \text{(B3)}$$

$$\mathcal{T}^{a(\rm II)}=i(\vec{\tau}_1+\vec{\tau}_2)^a\boldsymbol{k}\cdot\boldsymbol{\sigma}_1\times\boldsymbol{\sigma}_2, \quad \text{(B4)}$$

with $\boldsymbol{k}=\boldsymbol{k}_2=-\boldsymbol{k}_1$. The one-pion-exchange contribution including the vertex renormalization (loop corrections to the vertices) reads

$$\mathcal{W}_{1\pi}^{(\rm I)}=-\frac{1}{m_\pi^2-t}F_1^V(t),$$

$$\mathcal{W}_{1\pi}^{(\rm II)}=0, \quad \text{(B5)}$$

where $t\equiv k_0^2-\boldsymbol{k}^2\simeq-\boldsymbol{k}^2$, and $F_1^V(t)$ is the isovector Dirac form factor of the nucleon electromagnetic current. The phenomenologically determined $F_1^V(t)$ is of the dipole type

$$F_1^V(t)=\left(\frac{\Lambda^2}{\Lambda^2-t}\right)^2 \quad \text{(B6)}$$

with $\Lambda=840$ MeV. The HBχPT expression for $F_1^V(t)$ up to one-loop accuracy is given by

$$F_1^V(t)=1+\frac{c_3^R}{f_\pi^2}t-\frac{t}{16\pi^2 f_\pi^2}\left[\frac{1+3g_A^2}{2}K_0(t)-2(1+2g_A^2)K_2(t)\right]. \quad \text{(B7)}$$

The loop functions, K's, will be specified below. The constant c_3^R is determined by the nucleon charge radius [73].

$$c_3^R\frac{m_\pi^2}{f_\pi^2}=\frac{m_\pi^2}{6}\langle r^2\rangle_1^V\simeq 0.04784. \quad \text{(B8)}$$

We should mention here that $\mathcal{M}_{1\pi}$ in Eq. (B5) contains both $\mathcal{O}(Q^2)$ and $\mathcal{O}(Q^4)$ contributions. The $\mathcal{O}(Q^2)$ contributions can be obtained by replacing $F_1^V(t)$ by 1, while $[F_1^V(t)-1]$ is responsible for the $\mathcal{O}(Q^4)$ contributions. The two-pion-exchange contributions, which are also of $\mathcal{O}(Q^4)$, are given by

$$\mathcal{W}_{2\pi}^{(\mathrm{I})}=\frac{1}{16\pi^2 f_\pi^2}\left[-\frac{3g_A^2-2}{4}K_0(k^2)-\frac{1}{2}g_A^2K_1(k^2)\right]-\frac{1}{4f_\pi^2}\kappa_4^{(1)},$$

$$\mathcal{W}_{2\pi}^{(\mathrm{II})}=\frac{1}{16\pi^2 f_\pi^2}[2g_A^2K_0(k^2)]-\frac{1}{4f_\pi^2}\kappa_4^{(2)}, \quad \text{(B9)}$$

where $\kappa_4^{(1)}$ and $\kappa_4^{(2)}$ are unknown parameters [74]. The total two-body axial-charge operator is the sum of Eqs. (B5) and (B9):

$$\mathcal{W}^{(\mathrm{I})}=\mathcal{W}_{1\pi}^{(\mathrm{I})}+\mathcal{W}_{2\pi}^{(\mathrm{I})},$$

$$\mathcal{W}^{(\mathrm{II})}=\mathcal{W}_{1\pi}^{(\mathrm{II})}+\mathcal{W}_{2\pi}^{(\mathrm{II})}. \quad \text{(B10)}$$

The loop functions K's in the above are defined as

$$K_0(t)=\int_0^1 dz\ \ln\left[1-z(1-z)\frac{t}{m_\pi^2}\right],$$

$$K_1(t)=\int_0^1 dz\,\frac{-z(1-z)t}{m_\pi^2-z(1-z)t},$$

$$K_2(t)=\int_0^1 dz\,z(1-z)\ln\left[1-z(1-z)\frac{t}{m_\pi^2}\right]. \quad \text{(B11)}$$

The integrations over z can be done analytically, resulting in

$$K_0(t)=-2+\sigma\ln\left(\frac{\sigma+1}{\sigma-1}\right),$$

$$K_1(t)=1-\frac{\sigma^2-1}{2\sigma}\ln\left(\frac{\sigma+1}{\sigma-1}\right),$$

$$K_2(t)=-\frac{4}{9}+\frac{\sigma^2}{6}+\frac{\sigma(3-\sigma^2)}{12}\ln\left(\frac{\sigma+1}{\sigma-1}\right), \quad \text{(B12)}$$

with

$$\sigma\equiv\left(\frac{4m_\pi^2-t}{-t}\right)^{1/2}. \quad \text{(B13)}$$

APPENDIX C: REGULARIZATION AND THE CUTOFF

1. Fourier transform

Since SNPA employs coordinate-space representation, we need to Fourier transform the momentum-space expressions. In doing so, we must impose a cutoff to regularize the integral. The cutoff introduced here typically represents a scale that divides the low-energy degrees of freedom (which we choose to include explicitly) and the high-energy degrees of freedom (which we integrate out). How to implement cutoff into the theory is not unique, but physics should be independent of methods used insofar as the calculation is done consistently. This is a statement of renormalization group invariance. We now describe a particular cutoff scheme to be used here [75]. For the n_B-body current in momentum space $\boldsymbol{A}_{12\cdots n}^a=\boldsymbol{A}_{12\cdots n}^a(\boldsymbol{k}_1,\boldsymbol{k}_2,\cdots,\boldsymbol{k}_n)$, define its "Fourier transform" as

$$\tilde{\boldsymbol{A}}_{12\cdots n}^a\equiv\left[\prod_{l=1}^n\int\frac{d^3\boldsymbol{k}_l}{(2\pi)^3}e^{i\boldsymbol{k}_l\cdot\boldsymbol{r}_l}S_\Lambda(\boldsymbol{k}_l^2)\right]\times(2\pi)^3\delta^{(3)}(\boldsymbol{q}+\boldsymbol{k}_1+\boldsymbol{k}_2+\cdots+\boldsymbol{k}_n)\boldsymbol{A}_{12\cdots n}^a, \quad \text{(C1)}$$

where $S_\Lambda(\boldsymbol{k}^2)$ is a regulator with a cutoff Λ, and the factor $(2\pi)^3\delta^{(3)}(\boldsymbol{q}+\boldsymbol{k}_1+\boldsymbol{k}_2+\cdots+\boldsymbol{k}_n)$ comes from momentum conservation. We employ here a regulator of the Gaussian type [76]

$$S_\Lambda(\boldsymbol{k}^2)=\exp\left(-\frac{\boldsymbol{k}^2}{2\Lambda^2}\right). \quad \text{(C2)}$$

For a one-body operator, the regulator plays no role, see Eq. (A3). Now for the two-body current Eq. (C1) gives [77]

$$\tilde{\boldsymbol{A}}_{12}^a=\int\frac{d^3\boldsymbol{k}}{(2\pi)^3}S_\Lambda^2(\boldsymbol{k}^2)e^{-i\boldsymbol{k}\cdot\boldsymbol{r}_{12}}\times\boldsymbol{A}_{12}^a(\boldsymbol{k}_1=-\boldsymbol{k},\ \boldsymbol{k}_2=\boldsymbol{k}). \quad \text{(C3)}$$

To simplify subsequent expressions, we will hereafter omit the tildes on the currents in the coordinate space representation, and define the following functions:

$$\delta_\Lambda^{(3)}(\boldsymbol{r})\equiv\int\frac{d^3\boldsymbol{k}}{(2\pi)^3}S_\Lambda^2(\boldsymbol{k}^2)e^{i\boldsymbol{k}\cdot\boldsymbol{r}},$$

$$y_{0\Lambda}(m,r)\equiv\int\frac{d^3\boldsymbol{k}}{(2\pi)^3}S_\Lambda^2(\boldsymbol{k}^2)e^{i\boldsymbol{k}\cdot\boldsymbol{r}}\frac{1}{\boldsymbol{k}^2+m^2},$$

$$y_{1\Lambda}(m,r) \equiv -\frac{1}{m}\frac{\partial}{\partial r} y_{0\Lambda}(m,r),$$

$$y_{2\Lambda}(m,r) \equiv \frac{1}{m^2} r \frac{\partial}{\partial r}\frac{1}{r}\frac{\partial}{\partial r} y_{0\Lambda}(m,r). \tag{C4}$$

These functions become the ordinary delta and Yukawa functions when Λ goes to infinity. We also use the abbreviation $y^{\pi}_{0\Lambda}(r) \equiv y_{0\Lambda}(m_\pi, r)$, and similarly for $y^{\pi}_{1\Lambda}(r)$ and $y^{\pi}_{2\Lambda}(r)$. The regularized delta and Yukawa functions read

$$\delta^{(3)}_{\Lambda}(\boldsymbol{r}) = \frac{\Lambda^3}{(4\pi)^{3/2}} \exp\left(-\frac{\Lambda^2 r^2}{4}\right), \tag{C5}$$

$$y_{0\Lambda}(m,r) = \frac{1}{4\pi r} e^{m^2/\Lambda^2} \frac{1}{2}\left[e^{-mr} \mathrm{erfc}\left(-\frac{\Lambda r}{2} + \frac{m}{\Lambda}\right) - (r \leftrightarrow -r)\right]. \tag{C6}$$

We are now ready to write down the $\nu=3$ two-body axial-vector current Eq. (A6) in coordinate space:

$$\begin{aligned} \boldsymbol{A}^{a;\nu 3}_{12}(1\pi) = {} & \frac{g_A}{2m_N f_\pi^2} \delta^{(3)}_{\Lambda}(\boldsymbol{r}_{12}) \left[\frac{1}{3}\hat{c}_3 (\boldsymbol{\mathcal{O}}^a_+ + \boldsymbol{\mathcal{O}}^a_-) \right. \\ & + \frac{2}{3}\left(\hat{c}_4 + \frac{1}{4}\right)\boldsymbol{\mathcal{O}}^a_\times \Big] - \frac{g_A m_\pi^2}{2m_N f_\pi^2}\Big[\boldsymbol{\mathcal{O}}^a_{\mathcal{P}} y^{\pi}_{1\Lambda}(r_{12}) \\ & + \left[\hat{c}_3 (\boldsymbol{\mathcal{T}}^a_+ + \boldsymbol{\mathcal{T}}^a_-) - \left(\hat{c}_4 + \frac{1}{4}\right)\boldsymbol{\mathcal{T}}^a_\times \right] y^{\pi}_{2\Lambda}(r_{12}) \\ & + \left[\frac{1}{3}\hat{c}_3 (\boldsymbol{\mathcal{O}}^a_+ + \boldsymbol{\mathcal{O}}^a_-) + \frac{2}{3}\left(\hat{c}_4 + \frac{1}{4}\right)\boldsymbol{\mathcal{O}}^a_\times \right] \\ & \times y^{\pi}_{0\Lambda}(r_{12}) \Big], \end{aligned} \tag{C7}$$

$$\boldsymbol{A}^{a;\nu 3}_{12}(2\pi) = \frac{g_A}{2m_N f_\pi^2} \delta^{(3)}_{\Lambda}(\boldsymbol{r}_{12}) [\hat{d}_1 (\boldsymbol{\mathcal{O}}^a_+ + \boldsymbol{\mathcal{O}}^a_-) + 2\hat{d}_2 \boldsymbol{\mathcal{O}}^a_\times], \tag{C8}$$

where the superscript $(i,\ j)$ are particle indices $r_{12} \equiv |\boldsymbol{r}_{12}|$ and $\hat{\boldsymbol{r}}_{12} \equiv \boldsymbol{r}_{12}/r_{12}$. In the above equations, we have defined the following two-body spin-isospin operators:

$$\boldsymbol{\mathcal{O}}^{i,a}_{\odot} \equiv (\vec{\tau}_1 \odot \vec{\tau}_2)^a (\boldsymbol{\sigma}_1 \odot \boldsymbol{\sigma}_2)^i,$$

$$\boldsymbol{\mathcal{T}}^{i,a}_{\odot} \equiv \left(\hat{r}^i_{12}\hat{r}^j_{12} - \frac{\delta^{ij}}{3}\right) \boldsymbol{\mathcal{O}}^{aj}_{\odot}, \tag{C9}$$

where $\odot = (+,-,\times)$ and

$$\boldsymbol{\mathcal{O}}^{i,a}_{\mathcal{P}} \equiv -\frac{1}{2m_\pi} (\vec{\tau}_1 \times \vec{\tau}_2)^a (\overline{\boldsymbol{p}^i_1} \boldsymbol{\sigma}_2 \cdot \hat{\boldsymbol{r}}_{12} + \overline{\boldsymbol{p}^i_2} \boldsymbol{\sigma}_1 \cdot \hat{\boldsymbol{r}}_{12}). \tag{C10}$$

Note that $\boldsymbol{\mathcal{O}}^{i,a}_{\mathcal{P}}$ is completely determined by Lorentz invariance. In terms of these seven operators, we can write *all* the two-body currents (including $\nu=3$ and $\nu=4$ contributions) as

$$\begin{aligned} \boldsymbol{A}^{i,a}_{12} = {} & -\sum_{\odot=+,-,\times} [F^C_{\odot}(r_{12}) \boldsymbol{\mathcal{O}}^{i,a}_{\odot} + F^T_{\odot}(r_{12}) \boldsymbol{\mathcal{T}}^{i,a}_{\odot}] \\ & - \frac{g_A m_\pi^2}{2m_N f_\pi^2} y^{\pi}_{1\Lambda}(r_{12}) \boldsymbol{\mathcal{O}}^{i,a}_{\mathcal{P}} + \frac{g_A}{2m_N f_\pi^2} \delta^{(3)}_{\Lambda}(\boldsymbol{r}_{12}) \\ & \times \left[\sum_{\odot=+,-,\times} \hat{d}_{\odot} \boldsymbol{\mathcal{O}}^{i,a}_{\odot} \right]. \end{aligned} \tag{C11}$$

We have separated out here the part proportional to $\delta^{(3)}_{\Lambda}(\boldsymbol{r})$. The dimensionless parameters $\hat{d}_{\odot}$ are given by $\hat{d}_{1,2}$ and (higher order) loop contributions as

$$\begin{aligned} \hat{d}_+ &\equiv \hat{d}_1 + \frac{1}{3}\hat{c}_3 - \frac{g_A^2 m_N m_\pi}{32\pi}(-3X_1 + 9X_{\sigma\tau} + 9X_\sigma - 3X_\tau), \\ \hat{d}_- &\equiv \hat{d}_1 + \frac{1}{3}\hat{c}_3 - \frac{g_A^2 m_N m_\pi}{32\pi}(-3X_1 + 9X_{\sigma\tau} - 9X_\sigma + 3X_\tau), \\ \hat{d}_\times &\equiv 2\left[\hat{d}_2 + \frac{1}{3}\left(\hat{c}_4 + \frac{1}{4}\right) + \frac{g_A^2 m_N m_\pi}{32\pi} X_{\sigma\tau} \right]. \end{aligned} \tag{C12}$$

The functions $F^{C,T}_{\odot}$ in Eq. (C11) are given by

$$\begin{aligned} F^C_+(r) = {} & \frac{g_A m_\pi^2}{2m_N f_\pi^2}\frac{\hat{c}^R_3}{3} y^{\pi}_{0\Lambda}(r) + \frac{g_A^3}{32\pi f_\pi^4}\left\{ \frac{1}{6}(3D_1 + k^2 D_2 - \tilde{D}_{1\pi})\frac{m_\pi^2}{m_\pi^2 + k^2} \right. \\ & \left. + \frac{1}{8}(3D_1 + k^2 D_2) + \frac{g_A^2}{64}(3D_3 - k^2 D_4 + 2k^2 D_5) \right\}_{\mathrm{FT}}(r), \\ F^C_-(r) = {} & \frac{g_A m_\pi^2}{2m_N f_\pi^2}\frac{\hat{c}^R_3}{3} y^{\pi}_{0\Lambda}(r) + \frac{g_A^3}{32\pi f_\pi^4}\left\{ \frac{1}{6}(3D_1 + k^2 D_2 - \tilde{D}_{1\pi})\frac{m_\pi^2}{m_\pi^2 + k^2} \right. \\ & \left. + \frac{1}{24}(3D_1 + k^2 D_2) + \frac{g_A^2}{64}\left(-D_3 + \frac{1}{3}k^2 D_4 + \frac{2}{3}k^2 D_5 \right) \right\}_{\mathrm{FT}}(r), \end{aligned}$$

$$F_{\times}^{C}(r)=\frac{g_A m_\pi^2}{2m_N f_\pi^2}\frac{2}{3}\left(\hat{c}_4^R+\frac{1}{4}\right)y_{0\Lambda}^{\pi}(r)+\frac{g_A^3}{32\pi f_\pi^4}\left\{\frac{2}{3}D_1-\frac{2}{3}(D_1-D_{1\pi})\frac{m_\pi^2}{m_\pi^2+k^2}\right\}_{\rm FT}(r) \tag{C13}$$

and

$$F_{+}^{T}(r)=\frac{g_A m_\pi^2}{2m_N f_\pi^2}\hat{c}_3^R y_{2\Lambda}^{\pi}(r)+\frac{g_A^3}{32\pi f_\pi^4}\left\{\frac{1}{2}(3D_1+k^2D_2-\tilde{D}_{1\pi})\frac{1}{m_\pi^2+k^2}+\frac{1}{4}D_2+\frac{g_A^2}{64}(-6D_4+3D_5)\right\}_{\rm FT}(r),$$

$$F_{-}^{T}(r)=\frac{g_A m_\pi^2}{2m_N f_\pi^2}\hat{c}_3^R y_{2\Lambda}^{\pi}(r)+\frac{g_A^3}{32\pi f_\pi^4}\left\{\frac{1}{2}(3D_1+k^2D_2-\tilde{D}_{1\pi})\frac{1}{m_\pi^2+k^2}-\frac{1}{4}D_2+\frac{g_A^2}{64}(2D_4+D_5)\right\}_{\rm FT}(r),$$

$$F_{\times}^{T}(r)=-\frac{g_A m_\pi^2}{2m_N f_\pi^2}\left(\hat{c}_4^R+\frac{1}{4}\right)y_{2\Lambda}^{\pi}(r)+\frac{g_A^3}{32\pi f_\pi^4}\left\{\frac{D_1-D_{1\pi}}{m_\pi^2+k^2}\right\}_{\rm FT}^{T}(r), \tag{C14}$$

where $k\equiv|\boldsymbol{k}|$, $D_i=D_i(k)$ and

$$\{f(k^2)\}_{\rm FT}(r)\equiv\int\frac{d^3\boldsymbol{k}}{(2\pi)^3}S_\Lambda^2(\boldsymbol{k}^2)e^{-i\boldsymbol{k}\cdot\boldsymbol{r}}f(k^2),$$

$$\{f(k^2)\}_{\rm FT}^{T}(r)\equiv r\frac{\partial}{\partial r}\frac{1}{r}\frac{\partial}{\partial r}\int\frac{d^3\boldsymbol{k}}{(2\pi)^3}S_\Lambda^2(\boldsymbol{k}^2)e^{-i\boldsymbol{k}\cdot\boldsymbol{r}}\ f(k^2).$$

The explicit results of Fourier transformation of $D_i(k)$ and $k^2D_i(k)$ are given by ("$\rightarrow$" denotes Fourier transformation):

$$D_1\rightarrow-\frac{m_\pi^2}{2\pi r^2}\int_0^1 dz\,K_2(x),$$

$$D_2\rightarrow\frac{1}{2\pi r^2}\int_0^1 dz\,z\bar{z}\,xK_1(x),$$

$$D_3\rightarrow\frac{m_\pi^2}{2\pi r^2}\int_0^1 dz\,[6K_2(x)+xK_1(x)],$$

$$D_4\rightarrow\frac{1}{2\pi r^2}\int_0^1 dz\,[z\bar{z}\,x^2K_0(x)+(6z\bar{z}-1)xK_1(x)],$$

$$D_5\rightarrow\frac{1}{2\pi r^2}\int_0^1 dz\,xK_1(x) \tag{C15}$$

and

$$\boldsymbol{k}^2D_2=D_1-m_\pi^2D_5\rightarrow-\frac{m_\pi^2}{2\pi r^2}\int_0^1 dz\,[K_2(x)+xK_1(x)],$$

$$\boldsymbol{k}^2D_4\rightarrow-\frac{m_\pi^2}{2\pi r^2}\int_0^1 dz\left[\frac{6z\bar{z}-1}{z\bar{z}}[2xK_1(x)+K_2(x)]+x^2K_0(x)-xK_1(x)\right],$$

$$\boldsymbol{k}^2D_5\rightarrow-\frac{m_\pi^2}{2\pi r^2}\int_0^1 dz\,\frac{1}{z\bar{z}}[2xK_1(x)+K_2(x)], \tag{C16}$$

where

$$x\equiv\frac{m_\pi r}{\sqrt{z\bar{z}}}. \tag{C17}$$

Next we turn to the three-body currents of Eq. (A17). The Fourier-transformed three-body current has the form

$$\boldsymbol{A}_{123}^{a}=-\sum_{\rm cycle(123)}\frac{g_A^3}{16f_\pi^4}(2\tau_1^a\vec{\tau}_2\cdot\vec{\tau}_3-\tau_2^a\vec{\tau}_3\cdot\vec{\tau}_1-\tau_3^a\vec{\tau}_1\cdot\vec{\tau}_2)\boldsymbol{I}_{123} \tag{C18}$$

with

$$\boldsymbol{I}_{123}\equiv\left[\prod_{i=l}^{3}\int\frac{d^3\boldsymbol{k}_l}{(2\pi)^3}e^{i\boldsymbol{k}_l\cdot\boldsymbol{r}_l}e^{-\boldsymbol{k}_l^2/2\Lambda^2}\right]\times(2\pi)^3\delta^{(3)}(\boldsymbol{k}_1+\boldsymbol{k}_2+\boldsymbol{k}_3)\times\left(\boldsymbol{\sigma}_1-\frac{4}{3}\frac{\boldsymbol{k}_1\boldsymbol{\sigma}_1\cdot\boldsymbol{k}_1}{\boldsymbol{k}_1^2+m_\pi^2}\right)\frac{\boldsymbol{\sigma}_2\cdot\boldsymbol{k}_2}{\boldsymbol{k}_2^2+m_\pi^2}\frac{\boldsymbol{\sigma}_3\cdot\boldsymbol{k}_3}{\boldsymbol{k}_3^2+m_\pi^2}.$$

The calculation of I_{123}^{i} is rather involved. We may start with exploiting the identity

$$(2\pi)^3\delta^{(3)}(\boldsymbol{k}_1+\boldsymbol{k}_2+\boldsymbol{k}_3)=\int d^3\boldsymbol{x}e^{i\boldsymbol{x}\cdot(\boldsymbol{k}_1+\boldsymbol{k}_2+\boldsymbol{k}_3)} \tag{C19}$$

to arrive at

$$I^i_{123} = -\frac{4m_\pi^4}{3}\int d^3\boldsymbol{x}\left[\frac{5}{12m_\pi^2}\sigma_1^i\delta^{(3)}_{\Lambda}(\boldsymbol{x}) + \sigma_1^i y^{\pi}_{0\bar{\Lambda}}(|\boldsymbol{x}|) - \left(\hat{x}^i\hat{x}^j - \frac{\delta^{ij}}{3}\right)\sigma_1^j y^{\pi}_{2\bar{\Lambda}}(|\boldsymbol{x}|)\right]\frac{\boldsymbol{\sigma}_2\cdot(\boldsymbol{x}+\boldsymbol{r}_{12})}{|\boldsymbol{x}+\boldsymbol{r}_{12}|} \times y^{\pi}_{1\bar{\Lambda}}(|\boldsymbol{x}+\boldsymbol{r}_{12}|)\frac{\boldsymbol{\sigma}_3\cdot(\boldsymbol{x}+\boldsymbol{r}_{13})}{|\boldsymbol{x}+\boldsymbol{r}_{13}|}y^{\pi}_{1\bar{\Lambda}}(|\boldsymbol{x}+\boldsymbol{r}_{13}|),$$

with $\bar{\Lambda}\equiv\sqrt{2}\Lambda$. This representation is nicely transparent, and the resulting integrand is nonoscillatory and rapidly damping. The remaining integration can be done by means of a Monte Carlo simulation with Metropolis random walks.

2. The parameter $\hat{d}^R$

Up to N^{3}LO, unknown parameters occur only in $\boldsymbol{A}$. At N^{4}LO, several unknown parameters appear in both $\boldsymbol{V}$ and A_0, but no new parameters appear in $\boldsymbol{A}$. By the chiral filter argument, one can ignore the N^{4}LO terms in both $\boldsymbol{V}$ and A_0 while going to N^{4}LO in $\boldsymbol{A}$. Thus, up to N^{4}LO, the only genuinely unknown parameters reside in $\boldsymbol{A}$. The crucial observation is that up to N^{4}LO, there is effectively only one constant $\hat{d}^R$ that governs the GT amplitudes of all the cases under consideration. The argument goes as follows.

The two parameters, $\hat{d}_1$ and $\hat{d}_2$, and the four X's can be combined into three unknown parameters $\hat{d}_{\pm,\times}$ that reflect short-range physics. It is the Fermi-Dirac statistics that reduces the number of unknowns from three to one. To see this, let Ξ^σ and Ξ^τ be the exchange operators in spin and isospin spaces, respectively; $\Xi^\sigma=\frac{1}{2}(1+\boldsymbol{\sigma}_1\cdot\boldsymbol{\sigma}_2)$, and $\Xi^\tau=\frac{1}{2}(1+\vec{\tau}_1\cdot\vec{\tau}_2)$. An explicit calculation gives the identity $\boldsymbol{\sigma}_1\times\boldsymbol{\sigma}_2=i(\boldsymbol{\sigma}_1-\boldsymbol{\sigma}_2)\Xi^\sigma$, and likewise for $\vec{\tau}_1\times\vec{\tau}_2$. Now, the Fermi-Dirac statistics requires that $\Xi^r\Xi^\sigma\Xi^\tau=-1$, where Ξ^r is the Majorana exchange operator that exchanges the orbital coordinates $\boldsymbol{r}_1$ and $\boldsymbol{r}_2$. As a result,

$$\mathcal{O}^{i,a}_{\times} = -\mathcal{O}^{i,a}_{-}\Xi^\sigma\Xi^\tau = \mathcal{O}^{i,a}_{-}\Xi^r. \tag{C20}$$

When multiplied by the delta function $\delta^{(3)}(\boldsymbol{r})$, the operators are nonvanishing only for the $L=0$ states, which then implies $S+T=1$. Acting on $L=0$ states, $\mathcal{O}^{i,a}_{+}$ is identically zero, since either spin or isospin must be equal to zero. Furthermore, the $L=0$ states are eigenstates of the operator Ξ^r with eigenvalue 1, so that $\mathcal{O}^{i,a}_{-}$ becomes identical to $\mathcal{O}^{i,a}_{\times}$. Thus we are left with only one unknown parameter

$$\hat{d}^R \equiv \hat{d}_- + \hat{d}_\times = \hat{d}_1 + 2\hat{d}_2 + \frac{1}{3}\hat{c}_3 + \frac{2}{3}\hat{c}_4 + \frac{1}{6}. \tag{C21}$$

The above argument is not strictly valid for the cutoff delta function $\delta^{(3)}_{\Lambda}(\boldsymbol{r})$, which has a finite (albeit very small) range $\sim\Lambda^{-1}$. However, deviations from the ordinary delta function case is higher order in chiral counting and hence can be ignored.

Since $\hat{d}_R$ accompanies the regularized delta-function $\delta^{(3)}_{\Lambda}(\boldsymbol{r})$, its contribution depends on Λ rather strongly. However, the renormalization-group invariance of EFT requires that this sensitivity to Λ should be compensated by the contributions of the remaining terms. Since the single-particle piece of $\boldsymbol{A}$ has no Λ dependence, and since all the currents other than $\boldsymbol{A}$ have only weak Λ dependence, this compensation must occur between the finite-range two-body GT and the regularized delta-function term. This has been indeed verified in our calculation over a wide range of Λ (500–800 MeV) although, as mentioned above, the results for the 800 MeV cutoff should be viewed with caution.

[1] For a recent review, see, for example, J. Carlson and R. Schiavilla, Rev. Mod. Phys. **70**, 743 (1998).

[2] G.E. Brown and M. Rho (unpublished).

[3] G.E. Brown and M. Rho, Phys. Rev. Lett. **66**, 2720 (1991).

[4] S.K. Bogner, T.T.S. Kuo, A. Schwenk, D.R. Entem, and R. Machleidt, nucl-th/0108041; S.K. Bogner, A. Schwenk, T.T.S. Kuo, and G.E. Brown, nucl-th/0111042.

[5] A. Schwenk, B. Friman, and G.E. Brown, Nucl. Phys. **A703**, 745 (2002).

[6] T.-S. Park, L.E. Marcucci, R. Schiavilla, M. Viviani, A. Kievsky, S. Rosati, K. Kubodera, D.-P. Min, and M. Rho, nucl-th/0106025.

[7] T.-S. Park, L.E. Marcucci, R. Schiavilla, M. Viviani, A. Kievsky, S. Rosati, K. Kubodera, D.-P. Min, and M. Rho, nucl-th/0107012.

[8] J.N. Bahcall, Phys. Rep. **333**, 47 (2000), and references therein.

[9] R. Escribano, J.-M. Frere, A. Gevaert, and D. Monderen, Phys. Lett. B **444**, 397 (1998).

[10] A more modern and complete discussion on this observation has recently been given by Ananyan, Serot, and Walecka [11].

[11] S.M. Ananyan, B.D. Serot, and J.D. Walecka, Phys. Rev. C **66**, 055502 (2002).

[12] K. Kubodera, J. Delorme, and M. Rho, Phys. Rev. Lett. **40**, 755 (1978); M. Rho, *ibid.* **66**, 1275 (1991).

[13] G.E. Brown and M. Rho, Phys. Rep. **363**, 85 (2002); hep-ph/0103102.

[14] T.-S. Park, D.-P. Min, and M. Rho, Phys. Rev. Lett. **74**, 4153 (1995); Nucl. Phys. **A596**, 515 (1996).

[15] T.-S. Park, D.-P. Min, and M. Rho, Phys. Rep. **233**, 341 (1993); T.-S. Park, I.S. Towner, and K. Kubodera, Nucl. Phys. **A579**, 381 (1994).

[16] J. Carlson, D.O. Riska, R. Schiavilla, and R.B. Wiringa, Phys. Rev. C **44**, 619 (1991).

[17] R. Schiavilla, R.B. Wiringa, V.R. Pandharipande, and J. Carlson, Phys. Rev. C **45**, 2628 (1992).

[18] L.E. Marcucci, R. Schiavilla, M. Viviani, A. Kievsky, S. Rosati, and J.F. Beacom, Phys. Rev. C **63**, 015801 (2001).

[19] J.N. Bahcall, hep-ex/0002018; J.N. Bahcall and P.I. Krastev,

Phys. Lett. B **436**, 243 (1998).
[20] T.-S. Park, K. Kubodera, D.-P. Min, and M. Rho, Nucl. Phys. **A684**, 101 (2001); see also nucl-th/9904053.
[21] An alternative approach, which however, is in line with our viewpoint, has been discussed by Ananyan, Serot, and Walecka [11].
[22] S. Weinberg, Phys. Lett. B **251**, 288 (1990); Nucl. Phys. **B363**, 3 (1991); Phys. Lett. B **295**, 114 (1992).
[23] Although the same approach can be applied to *n*-body currents ($n \geqslant 2$), we concentrate here on the dominant 2B currents.
[24] T.-S. Park, K. Kubodera, D.-P. Min, and M. Rho, Phys. Lett. B **472**, 232 (2000).
[25] S.R. Beane, V. Bernard, T.-S.H. Lee, and U.-G. Meißner, Phys. Rev. C **57**, 424 (1998); S.R. Beane, V. Bernard, T.-S.H. Lee, U.-G. Meißner, and U. van Kolck, Nucl. Phys. **A618**, 381 (1997).
[26] T.-S. Park, K. Kubodera, D.-P. Min, and M. Rho, Astrophys. J. **507**, 443 (1998).
[27] R. Schiavilla *et al.*, Phys. Rev. C **58**, 1263 (1998).
[28] The cutoff specifies not just the relevant degrees of freedom but also their momentum/energy content. This should be understood in what follows although we do not always mention it.
[29] D.E. Groom *et al.*, Particle Data Group, Eur. Phys. J. C **15**, 1 (2000).
[30] V. Bernard, N. Kaiser, and U.-G. Meißner, Nucl. Phys. **A615**, 483 (1997).
[31] T.D. Cohen, J.L. Friar, G.A. Miller, and U. van Kolck, Phys. Rev. C **53**, 2661 (1996).
[32] Our definition of the pion field here is different from that used in Ref. [31]; we have changed the sign of the pion field. Furthermore, we employ here manifestly Lorentz-invariant and chiral-invariant interactions.
[33] For convenience, a chiral order corresponding to ν is often referred to as N$^{\nu}$LO; $\nu=1$ corresponds to NLO (next-to-leading order), $\nu=2$ to N^{2}LO (next-to-next-to-leading order), and so on.
[34] Eq. (14) holds only for *gentle* processes wherein the energy transfer to the leptonic pair is much smaller than m_π; the processes considered in this paper are gentle. If the energy transfer becomes comparable to m_π, then the typical momentum scale becomes $Q \sim \sqrt{m_N m_\pi}$, and hence one should expect a much slower convergence of chiral expansion.
[35] For small but finite values of $\boldsymbol{q} \neq \boldsymbol{0}$, there are slight deviations from this chart; for instance, for all the four cases in the table, there arise one-body contributions at NLO and at higher orders. However, these deviations are not significant in our case, which involves very small values of $\boldsymbol{q}$.
[36] T.-S. Park, H. Jung, and D.-P. Min, Phys. Lett. B **409**, 26 (1997).
[37] V. Bernard, N. Kaiser, and U.-G. Meißner, Nucl. Phys. **B457**, 147 (1995).
[38] A sign error made in the expression for $\hat{d}^R$ in PKMR98 has been corrected here.
[39] The masses of the light-quark vector mesons (ρ and ω) are less than 800 MeV; therefore, with the use of $\Lambda = 800$ MeV, an accurate description of certain observables might require the explicit presence of the vector mesons, even though the probe energy/momentum in question is much smaller than 800 MeV. Thus the results with the cutoff $\Lambda = 800$ MeV should be taken with some caution.
[40] L.E. Marcucci, R. Schiavilla, M. Viviani, A. Kievsky, and S. Rosati, Phys. Rev. Lett. **84**, 5959 (2000).
[41] M. Viviani, A. Kievsky, and S. Rosati, Few-Body Syst. **18**, 25 (1995).
[42] M. Viviani, S. Rosati, and A. Kievsky, Phys. Rev. Lett. **81**, 1580 (1998).
[43] R.B. Wiringa, V.G.J. Stoks, and R. Schiavilla, Phys. Rev. C **51**, 38 (1995).
[44] B.S. Pudliner, V.R. Pandharipande, J. Carlson, and R.B. Wiringa, Phys. Rev. Lett. **74**, 4396 (1995).
[45] M. Kamionkowski and J.N. Bahcall, Astrophys. J. **420**, 884 (1994).
[46] The subscript pp has been added here to avoid confusion with the cutoff parameter Λ.
[47] J.C. Hardy, I.S. Towner, V.T. Koslowsky, E. Hagberg, and H. Schmeing, Nucl. Phys. **A509**, 429 (1990).
[48] S. Fukuda *et al.*, Phys. Rev. Lett. **86**, 5651 (2001).
[49] See below for a possible caveat on the given error estimate.
[50] The earlier studies [16,17] were based on less accurate variational wave functions than used here and in MSVKRB; furthermore they did not include *P*-wave capture contributions, which account for $\approx 40\%$ of the total *S* factor.
[51] J.N. Bahcall, M.H. Pinsonneault, and S. Basu, Astrophys. J. **555**, 990 (2001); astro-ph/0010346.
[52] T.-S. Park, K. Kubodera, D.-P. Min, and M. Rho (unpublished).
[53] J.L. Forest, V.R. Pandharipande, S.C. Pieper, R.B. Wiringa, R. Schiavilla, and A. Arriaga, Phys. Rev. C **54**, 646 (1996).
[54] J.-W. Chen, G. Rupak, and M.J. Savage, Phys. Lett. B **464**, 1 (1999).
[55] T.-S. Park, K. Kubodera, D.-P. Min, and M. Rho, Phys. Rev. C **58**, 637 (1998).
[56] E. Epelbaum, W. Glöckle, A. Krüger, and U.-G. Meißner, Nucl. Phys. **A645**, 413 (1999).
[57] S.R. Beane, P.F. Bedaque, M.J. Savage, and U. van Kolck, Nucl. Phys. **A700**, 377 (2002); nucl-th/0104030.
[58] In general, the short-range contribution is represented by local zero-range terms in the Lagrangian, and thus various differences in the short-range region can be well compensated by a few (local) counterterms. This requires, however, the short-range contributions to be properly renormalized. Here we do this order by order in EFT*. More discussions are found in the text.
[59] S. Bogner, T.T.S. Kuo, L. Coraggio, A. Covello, and N. Itaco, nucl-th/0108040.
[60] D.B. Kaplan, M.J. Savage, and M.B. Wise, Phys. Lett. B **424**, 390 (1998); Nucl. Phys. **B534**, 329 (1998).
[61] S.R. Beane, P.F. Bedaque, W.C. Haxton, D.R. Phillips, and M.J. Savage, in *At the Frontier of Particle Physics – Handbook of QCD*, edited by M. Shifman (World Scientific, Singapore, 2001), Vol. 1, p. 133.
[62] X. Kong and F. Ravendal, Nucl. Phys. **A656**, 421 (1999); *ibid.* **A665**, 137 (2000); Phys. Lett. B **470**, 1 (1999); nucl-th/0004038; M. Butler and J.-W. Chen, nucl-th/0101017.
[63] P. F. Bedaque, H.W. Griesshammer, H.-W. Hammer, and G. Rupak, nucl-th/0207034.
[64] E. Epelbaum, W. Glöckle, and U.-G. Meißner, Nucl. Phys.

A671, 295 (2000); E. Epelbaum, H. Kamada, A. Nogga, H. Witala, W. Glöckle, and U.-G. Meißner, Phys. Rev. Lett. **86**, 4787 (2001); E. Epelbaum *et al.*, nucl-th/0109065, and references therein.

[65] *Formally*, the G_P term contributes at N^{2}LO. This is because $G_P(0)$ is of $\mathcal{O}(\Lambda_\chi^2/Q^2)$, reflecting the fact that the one-pion-exchange contribution to the pseudoscalar form factor is $G_P(q^2)=4g_A m_N^2/(m_\pi^2-q^2)$. But the numerical values of q for both the pp and triton beta decay processes are extremely small, i.e., $q\leqslant 0.9$ and $q\leqslant 0.5$ MeV, respectively. Thus the G_P term contribution is negligible, $\lesssim 0.01\%$ in the cross section. For the hep process, the maximum value of q is 19 MeV at threshold, and the correction due to the G_P term to the one-body GT matrix element can be about 1%, which is still too small to alter our estimation of the theoretical uncertainties.

[66] N. Fettes, U.-G. Meißner, and S. Steinberg, Nucl. Phys. **A640**, 199 (1998).

[67] M. Chemtob and M. Rho, Nucl. Phys. **A163**, 1 (1971).

[68] I.S. Towner, Phys. Rep. **155**, 263 (1987).

[69] E. Ivanov and E. Truhlik, Nucl. Phys. **A316**, 451 (1979); **A316**, 437 (1979).

[70] The one-body operators are not sensitive to these additional ingredients as long as the single-nucleon parameters are determined empirically. We note, however, that CRSW91 includes only the leading-order GT operator, $(\tau^a/2)g_A\boldsymbol{\sigma}$, without taking into account relativistic corrections.

[71] The pseudovector πNN coupling constant $f_{\pi NN}$ used in CRSW91 is related to the quantities used here as $f_{\pi NN}/m_\pi = g_{\pi NN}/2m_N = g_A/2f_\pi$. For the last equality, the Goldberger-Treiman relation has been used.

[72] Since g_ρ used in CRSW91 is half of the conventional one, the KSRF relation here reads $2(2g_\rho)^2 f_\pi^2 = m_\rho^2$, rather than $2g_\rho^2 f_\pi^2 = m_\rho^2$.

[73] Note that this c_3^R has nothing to do with the c's that appear in the GT operators. This confusing situation arises due to the lack of a unified system for labeling the coefficients in the chiral Lagrangian. In a chiral expansion $\mathcal{L}=\mathcal{L}_0+\mathcal{L}_1+\mathcal{L}_2+\cdots$, it was once common to use the letter b (c) to label the coefficients appearing in $\mathcal{L}_1$ ($\mathcal{L}_2$). Later, however, it has become more common to use the letter c to designate the coefficients that feature in $\mathcal{L}_1$, resulting in unfortunate confusions. In short, the above c_3^R is a coefficient in $\mathcal{L}_2$, while the c's appearing in the expression for the GT operator belong to $\mathcal{L}_1$.

[74] In fact, these are the only unknown parameters up to N^{4}LO. It turns out that due to the chiral filter mechanism, one can drop these terms when working to N^{4}LO for the GT operator.

[75] We illustrate our method for $\boldsymbol{A}$, but the same method is used for the other currents as well.

[76] Using a Gaussian cutoff can in principle upset the chiral counting even when graphs up to a definite chiral order (say ν) are considered. This counting mismatch, however, occurs at an order higher than ν, and furthermore the error committed is likely to be minimized by the regularization scheme we have adopted for the $\hat{d}^R$ counterterm.

[77] From here on, we shall specialize ourselves to the threshold limit $\boldsymbol{q}=\boldsymbol{0}$.